The Henryk Niewodniczański

INSTITUTE OF NUCLEAR PHYSICS

Polish Academy of Sciences

152 Radzikowskiego str., 31-342, Kraków, Poland

www.ifj.edu.pl/publ/reports/2006

Kraków, August 2006

REPORT No 1976/PH

Centrality in Hadron-Carbon, Hadron-Lead, and Lead-Lead Reactions at 158 GeV/c

Andrzej Rybicki

Abstract

A study of centrality in p+C, π+C, p+Pb, π+Pb, and Pb+Pb reactions is made. The analysis is performed by means of a simple geometrical model.

The mean number of elementary collisions, $< \nu >$, is estimated in minimum bias p+C reactions. For the specific case of the carbon nucleus, estimates on $< \nu >$ appear to depend strongly on assumed nuclear densities. Most realistic of the presented assumptions result in a value of $< \nu >= 1.71 \pm 0.05$. Additional quantities, like predictions for the total inelastic cross-section in p+C reactions, or the number of participants in minimum bias C+C collisions, are given.

The analysis is subsequently extended to minimum bias π+C, π+Pb, and p+Pb reactions. Estimates are given for the mean number of elementary collisions as well as for the contribution of single collisions $P(1)$. A comparison with experimental data is made.

Finally, the impact parameter dependence of p+Pb and Pb+Pb collisions is discussed.

In view of future studies, various aspects of the analysis are discussed in detail; a bibliography of used references is included.

This work was supported by the Polish State Committee for Scientific Research under grant no. 1 P03B 097 29

Contents

1 Introduction

This report contains a summary of several studies made on centrality of hadron-nucleus and nucleus-nucleus reactions at the top CERN SPS energy of 158 GeV/nucleon ($\sqrt{s}_{N+N} = 17.3$ GeV).

Its main aim is to provide a single, reasonably detailed source of information on several aspects of the nontrivial problem of determination of various centrality parameters: the mean number of elementary collisions $< \nu >$, the mean number of participating nucleons, and the probability $P(\nu)$ to hit a given number ν of nucleons (most of all the single hit contribution $P(1)$). The report is also supposed to provide quantitative information which will help the reader to get an idea on the collision geometry and on its dependence on impact parameter, or on the participating projectile and target. Finally, it is supposed to draw the reader's attention towards the importance of the nuclear profiles for centrality determination.

The present report concentrates on the problem of centrality *per se*: it discusses the centrality parameters as resulting from the assumed elementary cross-section, impact parameter and nuclear profile. The complicated matter of the relation between these parameters and different quantities used by SPS or RHIC experiments to define the centrality of non-minimum-bias samples (grey protons, energy deposited by charged particles, calorimetric information) [1, 2] is beyond its scope.

While the studies presented here have been made for the purpose of providing a background for analysis and interpretation of nuclear collision data from the NA49 experiment at the SPS [1], only a small part of the presented results specifically depends on the NA49 setup conditions. As such, the analysis presented here may serve for general considerations on hadron-nucleus and nucleus-nucleus collisions at beam energies of 158 GeV/nucleon.

Each of the three subsequent parts of this report constitutes in fact an independent analysis, performed on the basis of a specific motivation described separately for each part.

Part I
What is the Number of Collisions in Proton-Carbon Reactions?

2 Motivation

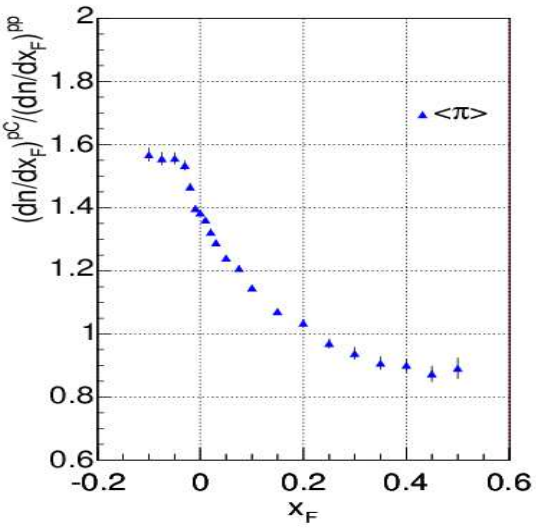

Figure 1: Ratio of pion production in minimum bias p+C relative to p+p collisions; the plot has been provided by Makariev [3].

The study presented in this Chapter is motivated by new experimental data communicated by Makariev [3] and presented in Fig. 1. The Figure shows the p+C/p+p pion production ratio as function of x_F (in the nucleon-nucleon c.m.s.). The measurements cover both the projectile and the target regions of p+C and p+p reactions. In view of the problem of unfolding the projectile and target contributions to pion production [4, 5], the question of the exact value of $< \nu >$ in p+C collisions becomes a very important issue.

The main difficulty of the study was to find reliable information about nuclear density profile in the relatively light ^{12}C nucleus. To provide an easy access to the information already found, and to the corresponding implications as far as centrality parameters are concerned, is the main purpose of this Chapter. The dependence of $< \nu >$ value on assumed nuclear density profiles appears surprisingly strong. To illustrate this, various less or more realistic approaches to the problem will be documented below. This will be done in detail in view of possible future work as well as for the author's own profit (self-documentation). As such, some redundancy of information is not to be avoided.

The remainder of this Chapter consists of a short description of the geometrical model used, of a discussion of the results obtained from simple-minded approaches to the nuclear density profiles, of the more realistic results obtained from more precise information on the charge distribution in the ^{12}C nucleus, of concluding remarks and an enumeration of the various remaining problems. On the basis of the present study estimates for the centrality parameters in p+C and C+C reactions are proposed. A reasonably detailed discussion of assumed error bars is included to give an idea of inherent uncertainties.

3 The Model

The study has been performed by means of a simple geometrical model simulation. The simulation produces spatial distributions of protons and neutrons using a given set of nuclear density functions (each nucleon is independently generated i.e. its position is not influenced by that of other nucleons belonging to the same nucleus). The simulation then assumes a uniform flux of proton projectiles to simulate minimum-bias p+C events. For each p+C event, a nucleon is defined as participant if it is crossed by at least one adverse nucleon within a transverse radius of less than 1 fm. This condition corresponds to the elementary nucleon-nucleon cross-section of 31.42 mb in good agreement with NA49 data [6]. It is important to stress that this elementary cross-section is assumed to be independent of the number of collisions undergone by the nucleon, and that no re-interaction with the spectator system is considered.

The number of collisions undergone by the projectile nucleon is then recorded event by event resulting in a prediction for $< \nu >$. At the same time the prediction for the total p+C inelastic cross-sections is calculated. As the simulation programs simultaneously generate proton and carbon projectiles, the number of participant pairs[1] and the mean number of collisions per participant in minimum bias C+C reactions will also be discussed in this Chapter.

4 Simple-Minded Approaches

For the carbon nucleus, experimental neutron over proton density information from antiprotonic atoms is not available [7], to the contrary of e.g. lead nuclei [8]. Therefore, for all simulations presented in this Chapter, the nuclear density profiles of protons and neutrons are assumed equal. The resulting problems will be addressed in Sec. 9.

4.1 Saxon-Woods

The most natural approach for a simple-minded $< \nu >$ calculation seems to use the Saxon-Woods parametrization, commonly used for heavier nuclei, and to try to extrapolate it down to carbon.

The Saxon-Woods (or Hofstadter et al. [9], or two-parameter Fermi [10, 11]) formula is:

$$\rho(r) = \frac{\rho_0}{1 + e^{(r-R)/z}}$$

where

- $\rho(r)$ is to be obviously understood as a spherically-symmetric $\rho(x, y, z) = \rho(\sqrt{x^2 + y^2 + z^2})$ density function.
- ρ_0 is the nuclear matter density at small values of r. As this is the plateau value for various nuclei (Fig. 2), it is also referred to as "constant nuclear matter density" and usually assumed equal to 0.17 nucleons per fm^3 [11].
- R is the $\rho(R) = \rho_0/2$ half-density value [9].
- z is a measure of surface thickness [9].

As described in [9, 11], for nuclei above $A \geq 40$ the Saxon-Woods parameters can be approximately described in a uniform fashion as $\rho_0 = 0.17$ fm^{-3}, $R = 1.07A^{\frac{1}{3}}$ fm, $z = 2.4/(4 \ln 3) = 0.546$ fm. It is to be underlined that carbon does *not* belong to the specified range.

A straight extrapolation down to ^{12}C gives $R = 2.450$ fm, $z = 0.546$ fm. Density integration over volume $\int \rho dV = 12$ results in $\rho_0 = 0.13070$ fm^{-3} which is significantly below the 0.17 expected. The obtained value of the nuclear root-mean-square radius is:

[1] Technically calculated as the mean number of projectile participants.

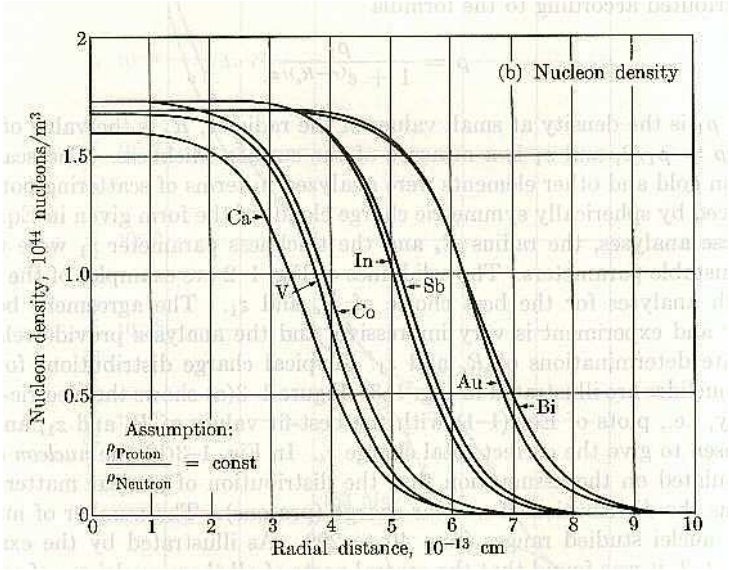

Figure 2: Nucleon densities as determined from electron scattering; the plot comes from [9]. Note the assumption on neutron distributions. The curves must evidently correspond to Saxon-Woods parameterizations rather than to experimental data (see discussion in Sec. 5).

$$< r^2 >^{\frac{1}{2}} = \sqrt{\frac{\int r^2 \rho(r) dV}{\int \rho(r) dV}} = 2.778 \text{ fm}$$

It is to be underlined that this is high as compared to $< r^2 >^{\frac{1}{2}}$ values obtained from experiment and discussed in Sec. 5, being on the order of 2.3-2.5 fm depending on definition.

The **results** of the simulation performed on the basis of such an assumed nuclear density are presented in Fig. 3. For minimum bias p+C reactions the obtained $< \nu >$ value is 1.520 $\pm$ 0.004[2]. The corresponding p+C inelastic cross-section is predicted to be 248 $\pm$ 1 mb. For minimum bias C+C reactions the predicted mean number of participant pairs is 3.15 $\pm$ 0.02 and the $< \nu >$ value is 1.516 $\pm$ 0.003.

For reference the numerical values of probabilities $P(\nu)$ are given below:

```
12C, extrapolated Saxon-Woods
              p+C       C+C
P(1)    =   0.6395    0.6422
P(2)    =   0.2418    0.2396
P(3)    =   0.0860    0.0866
P(4)    =   0.0257    0.0247
P(5)    =   0.0058    0.0057
P(6)    =   0.0011    0.0010
P(7)    =   0.0002    0.0002
```

It is in place to point out the strict similarity of $< \nu >$ and $P(\nu)$ in minimum bias p+C and C+C reactions. This also comes from all simulations made below; a comment will be made in Sec. 9.

[2]Unless explicitly specified, quoted errors are statistical only as resulting from the simulation. The treatment of statistical errors is described in Sec. 7.2.

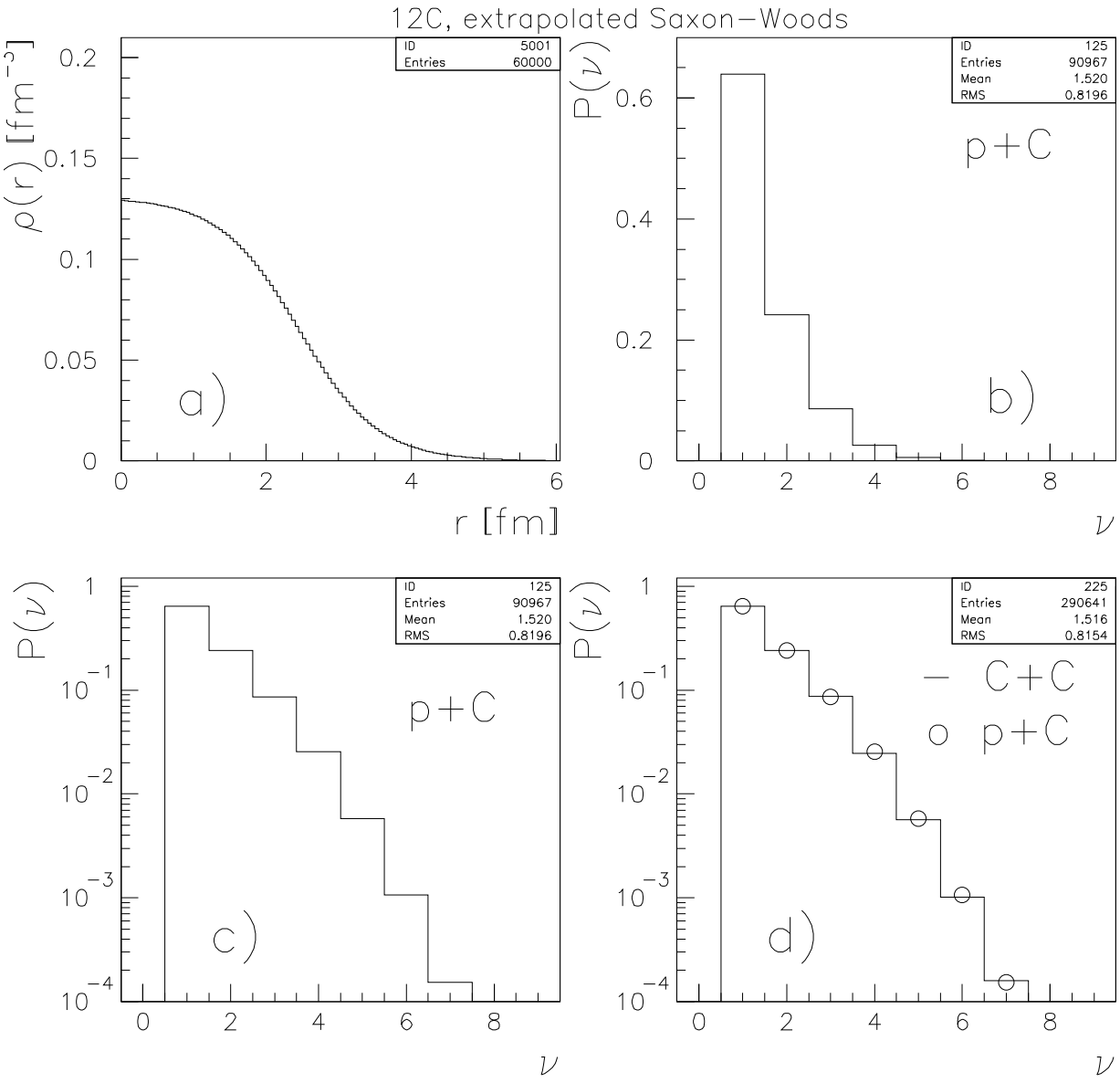

Figure 3: Results of the simulation assuming a Saxon-Woods density extrapolated down to carbon. a) absolutely normalized nucleon density profile, b) resulting probability distribution of $< \nu >$ in proton+carbon reactions, c) same on a log scale, d) $< \nu >$ distribution per participant in C+C reactions (histogram with displayed corresponding statistical parameters) compared to that in p+C reactions (circles).

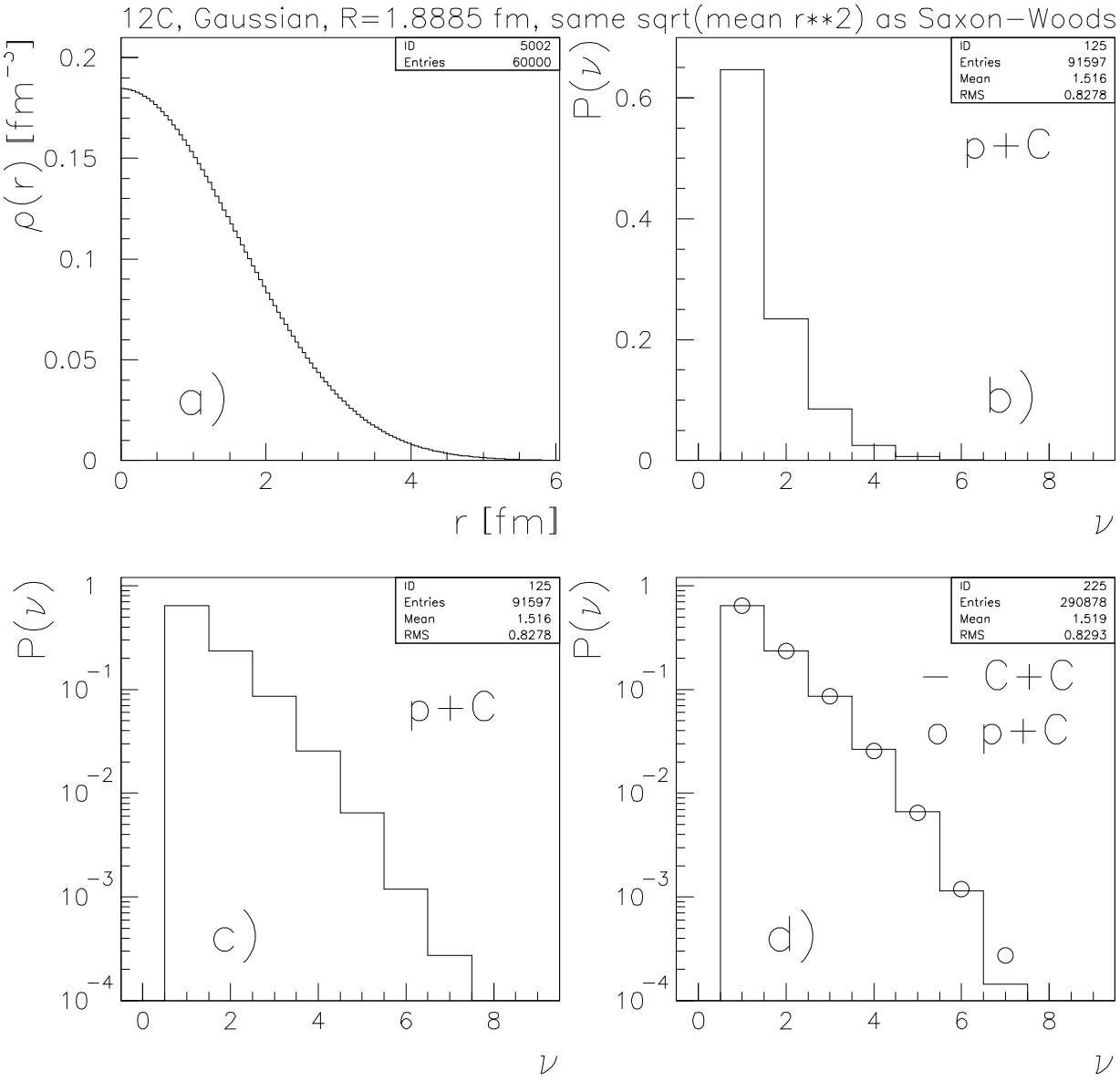

Figure 4: Results of the simulation assuming a Gaussian density profile. a) absolutely normalized nucleon density profile, b) resulting probability distribution of $< \nu >$ in proton+carbon reactions, c) same on a log scale, d) $< \nu >$ distribution per participant in C+C reactions (histogram with displayed corresponding statistical parameters) compared to that in p+C reactions (circles).

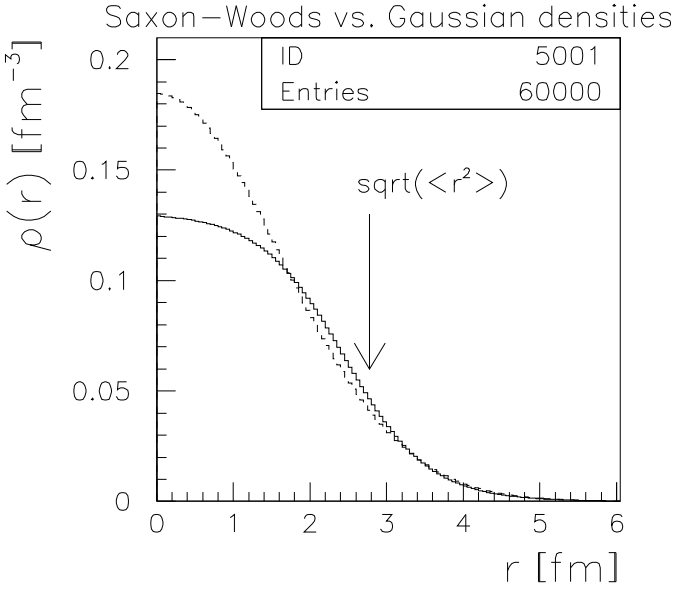

Figure 5: Comparison of used Saxon-Woods and Gaussian densities. The common value of $< r^2 >^{\frac{1}{2}} = 2.778$ fm is indicated by an arrow.

4.2 Gaussian

A suggestion has been made [12] that for light nuclei, the Saxon-Woods distribution is not appropriate (see above) and that a simple Gaussian is to be used instead, with the Gaussian width properly adjusted to the radius. Following that, the form of the nuclear density written below has been assumed:

$$\rho(r) = \rho^{\max} \exp\left(-\frac{r^2}{2(R/\sqrt{2\ln 2})^2}\right) = \rho^{\max} \exp\left(-\frac{r^2}{2(R/1.17741)^2}\right)$$

Here, the half-density radius has been adjusted to $R = 1.8885$ fm in order to have the distribution match the $< r^2 >^{\frac{1}{2}} = 2.778$ fm obtained above from the Saxon-Woods parametrization.

The **results** of the simulation performed on the basis of such an assumption are presented in Fig. 4. For minimum bias p+C reactions the obtained $< \nu >$ value is 1.516 ± 0.004. The p+C inelastic cross-section is predicted to be 249 ± 1 mb. For C+C reactions the predicted mean number of participant pairs is 3.14 ± 0.02 while the $< \nu >$ value is 1.519 ± 0.003.

For reference the numerical values of probabilities $P(\nu)$ are given below:

```
12C, Gaussian, R=1.8885 fm, same sqrt(mean r**2) as Saxon-Woods
              p+C       C+C
P(1)    =   0.6466    0.6451
P(2)    =   0.2341    0.2342
P(3)    =   0.0858    0.0863
P(4)    =   0.0255    0.0264
P(5)    =   0.0065    0.0066
P(6)    =   0.0012    0.0011
P(7)    =   0.0003    0.0001
```

It is to be noted that while the Saxon-Woods and Gaussian density profiles differ significantly in the region of $r < 1$ fm (Fig. 5), all the centrality parameters resulting from the two distributions characterized by the same $< r^2 >^{\frac{1}{2}}$ (that is, $< \nu >$, the $P(\nu)$ distribution, the inelastic cross-section, and the number of participant pairs in C+C reactions) are in fact very similar. A comment will be made in Sec. 9.

4.3 Sharp Sphere

The studies made in the two previous Sections have produced rather surprisingly low $< \nu >$ values. Therefore, the problem of what the upper limit of $< \nu >$ in proton+carbon collisions could be has been investigated. This has been done by assuming the ^{12}C nucleus as homogeneous sphere with the "constant nuclear density" $\rho_0 = 0.17$ fm^{-3}. While this simplest assumption could be expected to produce reasonable results for heavier nuclei with an extended plateau (Fig. 2), it becomes erroneous for the case of the carbon nucleus, as will be shown below.

By density integration over volume, one gets the sphere radius of 2.564 fm.

The **results** of the simulation performed on the basis of such an assumption are presented in Fig. 6. For minimum bias p+C reactions the obtained $< \nu >$ value is 1.941 ± 0.006. The p+C inelastic cross-section is predicted to be 196 ± 1 mb. For C+C reactions the predicted mean number of participant pairs is 4.10 ± 0.02 while the $< \nu >$ value is 1.933 ± 0.004.

For reference the numerical values of probabilities $P(\nu)$ are given below:

```
12C, Sharp homogeneous sphere with radius 2.56378 fm, rho=0.17 fm**-3
              p+C      C+C
P(1)   =   0.4605   0.4639
P(2)   =   0.2815   0.2810
P(3)   =   0.1565   0.1544
P(4)   =   0.0692   0.0692
P(5)   =   0.0242   0.0234
P(6)   =   0.0067   0.0067
P(7)   =   0.0013   0.0012
P(8)   =   0.0002   0.0001
```

4.4 Note

The conclusion from the analysis made in this Section is that simple-minded approaches to the nuclear density profile of ^{12}C fail to provide sufficient precision in determining the usual parameters characterizing the centrality of p+C or C+C collisions. The small size of the carbon nucleus results in a relatively strong dependence of the result on assumptions made. The spread of possible values is, at the least, 1.5-1.9 for the mean number of elementary collisions for both p+C and C+C, 195-250 mb for the p+C inelastic cross-section, and 3.1-4.1 for the number of participants in C+C reactions. More reliable input is necessary.

5 More Realistic Approaches: Charge Distributions

In the present Section the centrality parameters as issuing from density profiles deduced from charge distributions in ^{12}C are discussed. These charge distributions have been obtained from elastic electron scattering; in Sec. 5.2 the analysis has been additionally constrained by muonic x-ray data. The two different analyses presented in Secs. 5.1-5.2 have been quoted as "model-independent analyses", and indeed the two obtained charge density profiles are close. This is illustrated in Fig. 7.

It is to be mentioned that the dip in the density at $r = 0$ might possibly indicate a concentration of protons at some distance from the center of the nucleus due to Coulomb repulsion. However, it is to be indicated that non-monotonic structures emerge also from the data on density profiles in lead nuclei (Fig. 8), which makes the interpretation less clear.

In Secs. 5.1-5.2, the proton distribution is assumed to have the same shape as the charge distribution ($\rho_{proton}(r) = \rho_{charge}(r)$). A primitive attempt at proton unfolding will be made

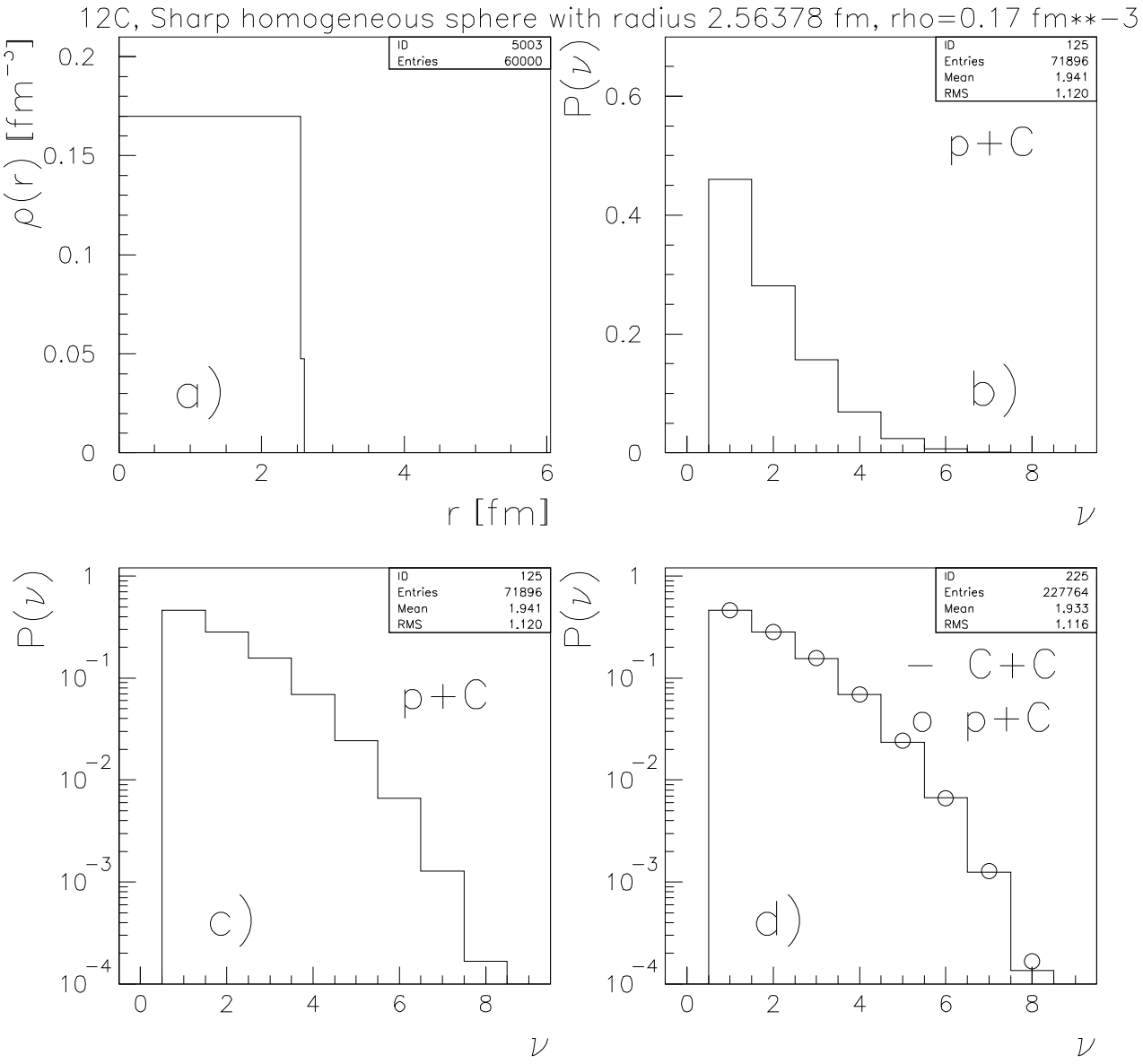

Figure 6: Results of the simulation assuming a homogeneous sphere. a) absolutely normalized nucleon density profile, b) resulting probability distribution of $< \nu >$ in proton+carbon reactions, c) same on a log scale, d) $< \nu >$ distribution per participant in C+C reactions (histogram with displayed corresponding statistical parameters) compared to that in p+C reactions (circles).

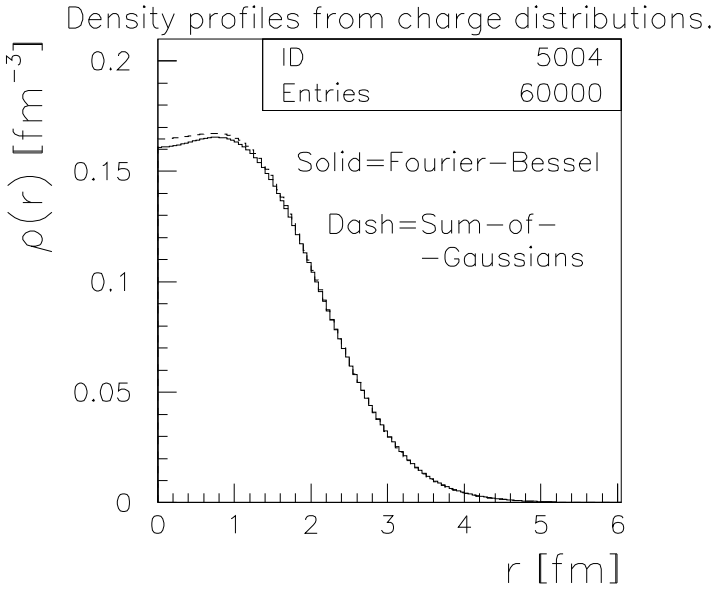

Figure 7: Comparison of nucleon density profiles directly obtained from charge distribution shapes [13, 14]. The corresponding values of $< r^2 >^{\frac{1}{2}}$ are respectively 2.478 fm (Fourier-Bessel) and 2.469 fm (Sum of Gaussians). Both nucleon densities are obtained by multiplying the charge density $\rho_{charge}(r)$ by 2.

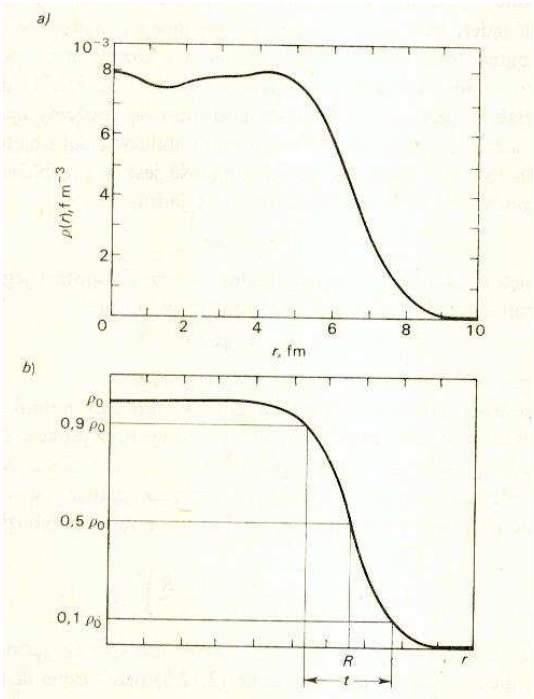

Figure 8: Proton density profiles in the ^{208}Pb nucleus, the Figure comes from [11]. Upper panel: result of model-independent analysis of electron scattering and muonic data. Lower panel: analytical (two-parameter Fermi) approximation. Note: personally, the author suspects the upper panel's vertical scale to be either wrong or explained incompletely.

in Sec. 6. All the studies are made with the assumption of equal proton and neutron density profiles:

$$\rho_{proton}(r) = \rho_{neutron}(r) = \frac{1}{2}\rho(r)$$

5.1 Fourier-Bessel Expansion

The model independent Fourier-Bessel analysis [15] uses an expansion of the nuclear charge density distribution:

$$\rho_{charge} = \sum_{n=1,n_{max}} a_n j_0(q_n r)$$

where

- a_n is directly related to measurable quantities;
- $j_0(q_n r) = \sin(q_n r)/(q_n r)$ is the zero-order spherical Bessel function;
- $q_n = n\pi/R_{cut}$;
- R_{cut} being a cutoff radius beyond which the charge density is assumed to be zero;
- n_{max} is the number of coefficients to be measured; it is determined by R_{cut} and by the maximum electron elastic scattering momentum transfer q_{max} given by experimental conditions.

It is to be underlined that the method is not completely assumption-free. Specifically, assumptions about the momentum transfer region $q > q_{max}$ are made [15].

The Fourier-Bessel analysis selected for the present study [13] describes the charge density profile by means of the following coefficients:

```
a( 1) = 1.5709 * (10.**(-2.))
a( 2) = 3.8610 * (10.**(-2.))
a( 3) = 3.6418 * (10.**(-2.))
a( 4) = 1.4293 * (10.**(-2.))
a( 5) =-4.4628 * (10.**(-3.))

a( 6) =-9.8420 * (10.**(-3.))
a( 7) =-6.6518 * (10.**(-3.))
a( 8) =-2.7066 * (10.**(-3.))
a( 9) =-5.6697 * (10.**(-4.))
a(10) =-2.7453 * (10.**(-4.))

a(11) =-1.7093 * (10.**(-4.))
a(12) = 1.2433 * (10.**(-4.))
a(13) =-4.8496 * (10.**(-5.))
a(14) = 1.5675 * (10.**(-5.))
a(15) =-4.5194 * (10.**(-6.))

a(16) = 1.1920 * (10.**(-6.))
a(17) =-2.9065 * (10.**(-7.))
a(18) = 6.5845 * (10.**(-8.))

Rcut = 8.0   ! fm
```

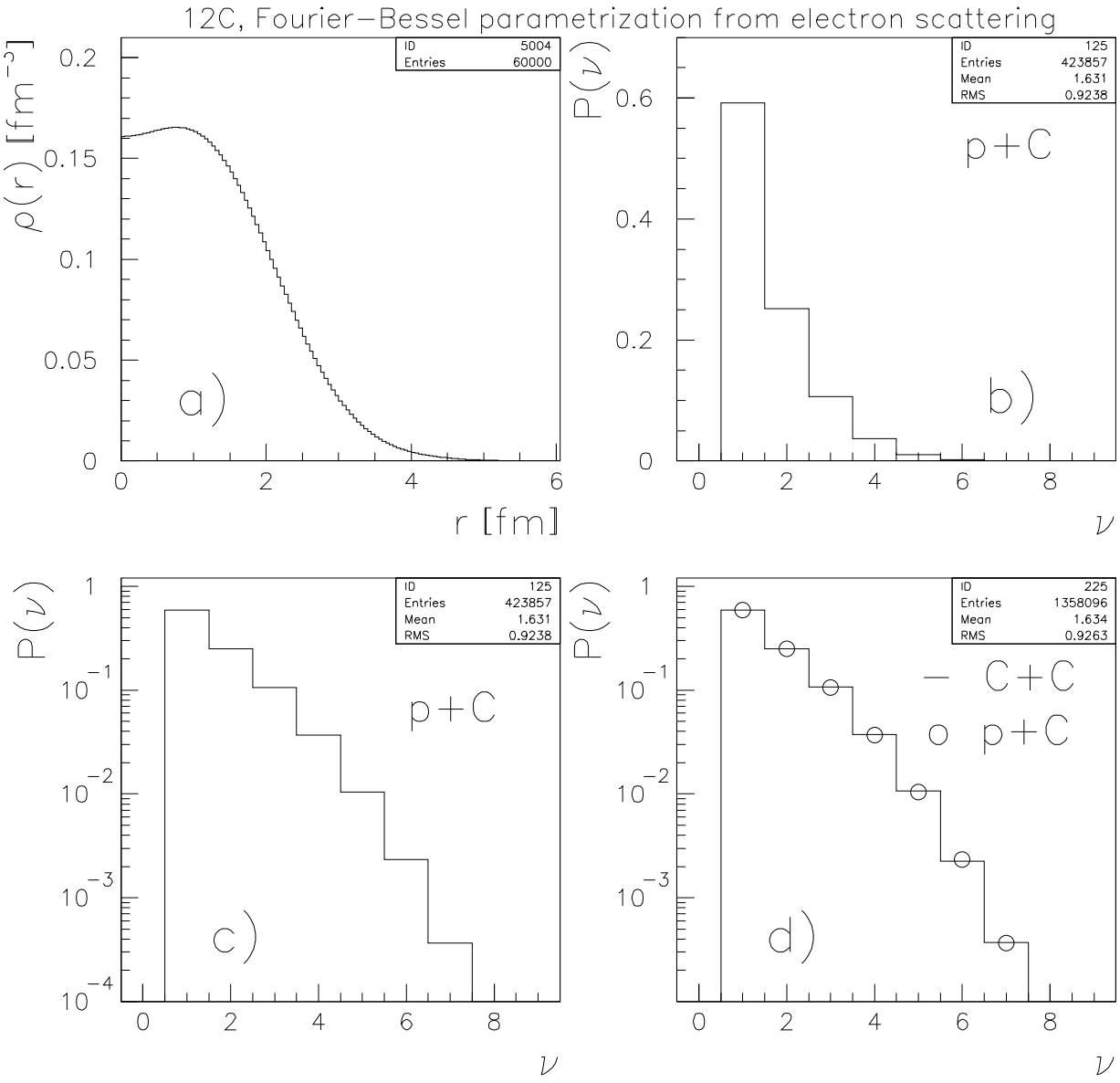

Figure 9: Results of the simulation assuming $\rho(r) = 2\rho_{charge}(r)$, where $\rho_{charge}(r)$ is obtained from a Fourier-Bessel analysis [13]. a) absolutely normalized nucleon density profile, b) resulting probability distribution of $< \nu >$ in proton+carbon reactions, c) same on a log scale, d) $< \nu >$ distribution per participant in C+C reactions (histogram with displayed corresponding statistical parameters) compared to that in p+C reactions (circles).

Assuming the shape of the nuclear density profile identical to that of the charge density distribution, one gets the **results** presented in Fig. 9. For minimum bias p+C reactions the obtained $< \nu >$ value is 1.631 ± 0.002. The p+C inelastic cross-section is predicted to be 231 ± 0.5 mb. For C+C reactions the predicted mean number of participant pairs is 3.45 ± 0.01 while the $< \nu >$ value is 1.634 ± 0.002.

For reference the numerical values of probabilities $P(\nu)$ are given below:

```
12C, Fourier-Bessel parametrization from electron scattering
             p+C      C+C
P(1)   =   0.5922   0.5913
P(2)   =   0.2514   0.2509
P(3)   =   0.1062   0.1069
P(4)   =   0.0370   0.0376
P(5)   =   0.0105   0.0107
P(6)   =   0.0023   0.0023
P(7)   =   0.0004   0.0004
P(8)   =   0.0001   0.0001
```

5.2 Sum of Gaussians

The model independent Sum-of-Gaussians analysis [16] uses the following expansion of the nuclear charge density distribution:

$$\rho_{charge}(r) = \sum_i A_i \left(\exp(-[(r-R_i)/\gamma]^2) + \exp(-[(r+R_i)/\gamma]^2) \right)$$

where the coefficients A_i are given by:

$$A_i = \frac{ZeQ_i}{2\pi^{\frac{3}{2}}\gamma^3(1+2R_i^2/\gamma^2)}$$

and

- positions R_i and amplitudes Q_i are fitted to the data;
  Q_i indicate the fraction of the total charge contained in each Gaussian ($\sum_i Q_i = 1$);
- the width of the Gaussians γ is chosen equal to the smallest width of the peaks in the nuclear radial wave functions calculated by the Hartree-Fock method. As only positive amplitudes are allowed, no structures narrower than γ can be created by interference.

The quoted reference specifies that the result of the Sum-of-Gaussians analysis is independent of the number of Gaussians, provided the latter is large enough.

The Sum-of-Gaussians analysis selected for the present study [14] is quoted in [16] as coming from electron scattering but constrained by muonic x-ray data. It provides following Gaussian positions and amplitudes, as well as the γ parameter obtained from the r.m.s. of the Gaussians, RP:

```
Ri( 1) = 0.0
Ri( 2) = 0.4
Ri( 3) = 1.0
Ri( 4) = 1.3
Ri( 5) = 1.7
Ri( 6) = 2.3
Ri( 7) = 2.7
```

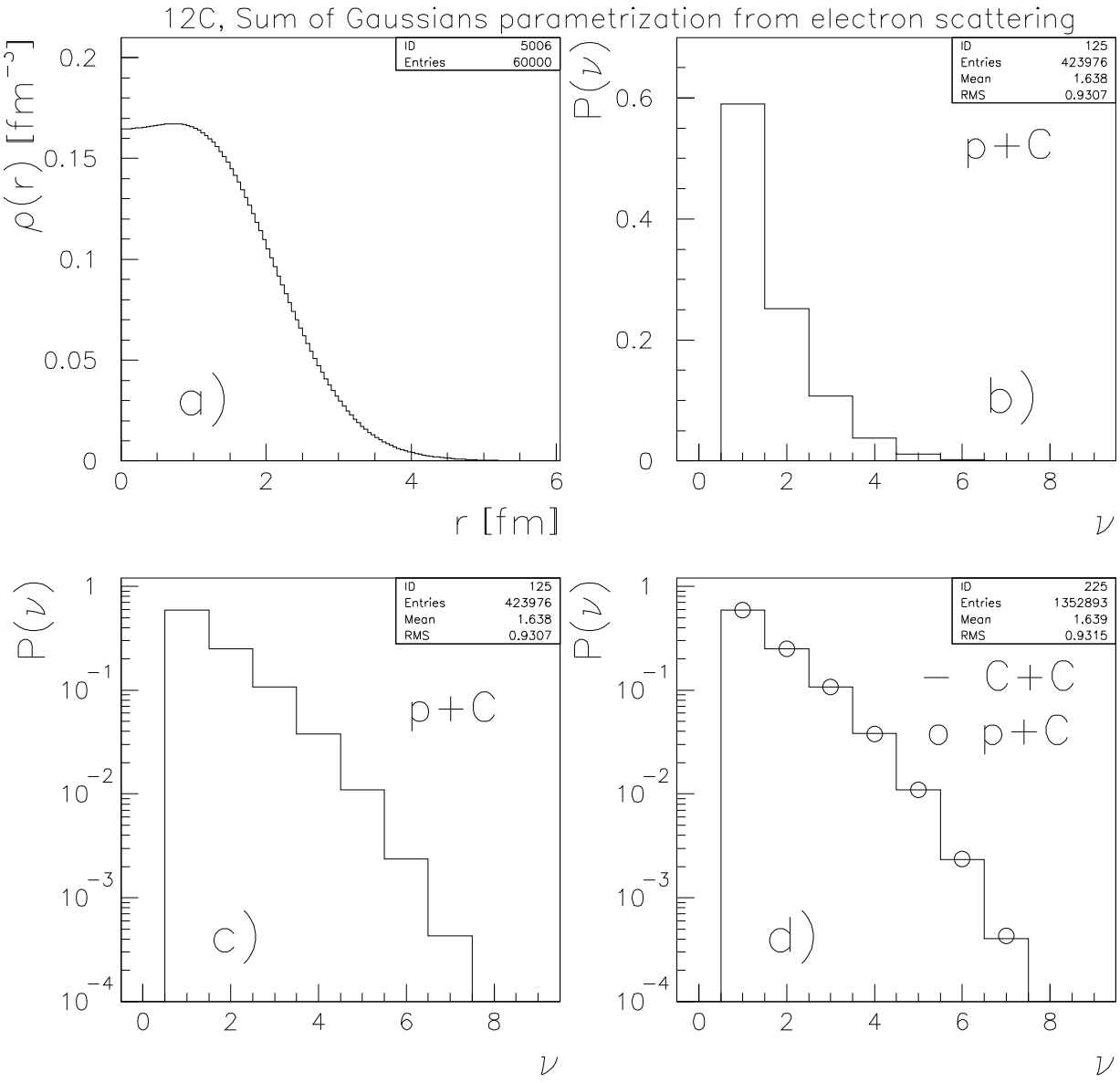

Figure 10: Results of the simulation assuming $\rho(r) = 2\rho_{charge}(r)$, where $\rho_{charge}(r)$ is obtained from a Sum-of-Gaussians analysis [14]. a) absolutely normalized nucleon density profile, b) resulting probability distribution of $< \nu >$ in proton+carbon reactions, c) same on a log scale, d) $< \nu >$ distribution per participant in C+C reactions (histogram with displayed corresponding statistical parameters) compared to that in p+C reactions (circles).

```
Ri( 8) = 3.5
Ri( 9) = 4.3
Ri(10) = 5.4
Ri(11) = 6.7

Qi( 1) = 0.016690
Qi( 2) = 0.050325
Qi( 3) = 0.128621
Qi( 4) = 0.180515
Qi( 5) = 0.219097
Qi( 6) = 0.278416
Qi( 7) = 0.058779
Qi( 8) = 0.057817
Qi( 9) = 0.007739
Qi(10) = 0.002001
Qi(11) = 0.000007

RP = 1.20   ! fm
gamma = RP / dsqrt( dble(1.5) )
```

Assuming the shape of the nuclear density profile identical to that of the charge density distribution, one gets the **results** presented in Fig. 10. For minimum bias p+C reactions the obtained $< \nu >$ value is 1.638 $\pm$ 0.002. The p+C inelastic cross-section is predicted to be 231 $\pm$ 0.5 mb. For C+C reactions the predicted mean number of participant pairs is 3.45 $\pm$ 0.01 while the $< \nu >$ value is 1.639 $\pm$ 0.002.

For reference the numerical values of probabilities $P(\nu)$ are given below:

```
12C, Sum of Gaussians parametrization from electron scattering
             p+C      C+C
P(1)   =   0.5897   0.5893
P(2)   =   0.2513   0.2514
P(3)   =   0.1073   0.1073
P(4)   =   0.0379   0.0382
P(5)   =   0.0109   0.0110
P(6)   =   0.0024   0.0023
P(7)   =   0.0004   0.0004
P(8)   =   0.0000   0.0001
```

It is seen that the two model-independent analyses (Fourier-Bessel, Sum-of-Gaussians) give indeed very similar centrality parameters for p+C and C+C reactions, as was to be expected from Fig. 7.

6 Attempt at Nucleon Unfolding

Even assuming that the proton and neutron distributions in the nucleus do not differ, the charge density distribution $\rho_{charge}(r)$ is not fully representative of the nucleon density distribution $\rho(r)$. As described in [10], the latter is related to the former by the spatial distribution of charge in the proton[3]:

[3]The volume integral written above is in fact eq. (2.11) from [10], rewritten in a more explicit way.

$$\rho_{charge}(r') = \int \rho_{proton}(r)\ \rho_{proton\ charge}(|r - r'|)\ dV$$

While it can be expected that this problem is less significant for large nuclei like ^{208}Pb, it will be important for small nuclei.

Following [10], the mean-square-radii of the two distributions are related by the following equation[4]:

$$< r^2_{charge} > \ = \ < r^2_{proton} > + < r^2_{proton\ charge} > \ = \ < r^2_{proton} > \ + \ 0.69 \quad \mathrm{fm}^2 \qquad (1)$$

In the present Section, the most primitive attempt at unfolding the proton density profiles from charge distributions is made. The proton density profile is obtained by linearly shrinking down the charge distribution following eq. (1), and the nucleon density profile is assumed equal to twice the proton density profile:

$$\rho(r) = 2\rho_{proton}(r) = 2a^3\rho_{charge}(ar) \qquad (2)$$

where

$$a = \frac{\sqrt{< r^2_{charge} >}}{\sqrt{< r^2_{proton} >}} = \frac{\sqrt{< r^2_{charge} >}}{\sqrt{< r^2_{charge} > -0.69}}$$

It is to be emphasized that this approach has evident weaknesses. Eq. (2) would be exactly correct only if the functions involved would be exact Gaussians which is not the case. On the other hand, the evident aim of the present exercise is to get some idea on the rough shape of resulting distributions in the situation where a remnant similarity to Gaussians still exists (Fig. 7), and to see the corresponding effect on $< \nu >$ and other centrality parameters. Finally, it is also hoped that with properly adjusted root-mean-square radii (equation (1)), the shape of the distribution will have only a secondary importance. This is what emerged from studies made in Secs. 4.1-4.2, where an evident difference between the Saxon-Woods profile and the Gaussian density distribution was also present (Fig. 5). The subject will have to be followed; a comment will be made in Sec. 9.

Following equation (2), the root-mean-square radii of the density profiles studied in Sec. 5 are modified in the following way:

```
rescaled Fourier-Bessel:      2.4777 fm -> 2.3343 fm,   a=1.061

rescaled Sum-of-Gaussians:    2.4693 fm -> 2.3254 fm,   a=1.062
```

The corresponding change of Fourier-Bessel and Sum-of-Gaussians density profiles is shown in Fig. 11. The large increase at small radii results in a nucleon density of up to 0.19-0.2, which seems a bit high relative to the standard $\rho_0 = 0.17$ fm^{-3} quoted in Sec. 4.1. In terms of number of nucleons, the corresponding excess is limited to a relatively small volume ($r < 1.5$ fm) and could be extremely grossly estimated to about 0.3 relative to the 12 nucleons present. It is to be further seen whether values of $\rho(r) = 0.19$ fm^{-3} can be considered as correct[5].

Altogether, the study presented below is to be treated as approximative and appropriately large error bands are to be assumed.

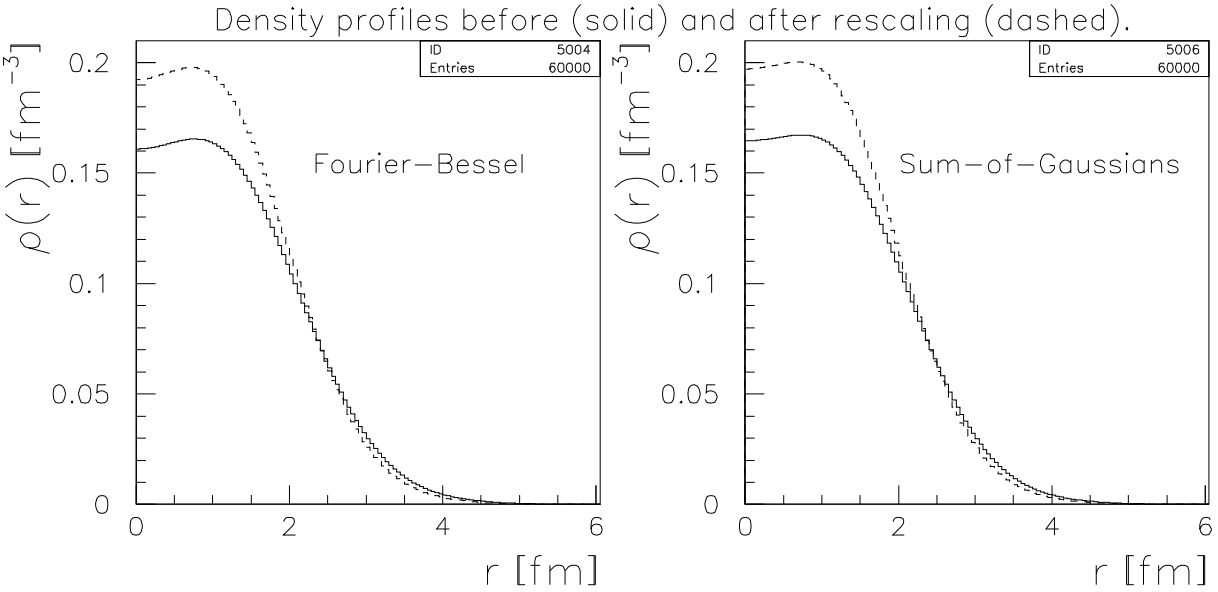

Figure 11: Comparison of nucleon density profiles used in Sec. 5 to the corresponding distributions obtained by the prescription (2).

6.1 Fourier-Bessel

Assuming the unfolded nucleon density profile as obtained from prescription (2) on the basis of the Fourier-Bessel charge distribution from Sec. 5.1, one gets the **results** presented in Fig. 12. For minimum bias p+C reactions the obtained $< \nu >$ value is 1.705 ± 0.002. The p+C inelastic cross-section is predicted to be 221 ± 0.5 mb. For C+C reactions the predicted mean number of participant pairs is 3.59 ± 0.01 while the $< \nu >$ value is 1.708 ± 0.002. This represents a change of respectively +0.074 collisions, -10 mb, +0.14 participant pairs, and +0.074 collisions relative to the non-unfolded spectra discussed in Sec. 5.1. This change remains at the level of a few percent but is non-negligible.

For reference the numerical values of probabilities $P(\nu)$ are given below:

```
 12C, Fourier-Bessel param. from electron scattering, rescaled to unfold
nucleons
                p+C       C+C
 P(1)    =    0.5647    0.5638
 P(2)    =    0.2540    0.2534
 P(3)    =    0.1168    0.1179
 P(4)    =    0.0457    0.0459
 P(5)    =    0.0144    0.0146
 P(6)    =    0.0037    0.0036
 P(7)    =    0.0006    0.0007
 P(8)    =    0.0001    0.0001
```

6.2 Sum of Gaussians

Assuming the unfolded nucleon density profile as obtained from prescription (2) on the basis of the Sum-of-Gaussians charge distributions (Sec. 5.2), one gets the **results** presented in Fig. 13. For minimum bias p+C reactions the obtained $< \nu >$ value is 1.713 ± 0.002. The p+C inelastic cross-section is predicted to be 220 ± 0.5 mb. For C+C reactions the predicted mean number

[4]Note that equation (1) implies that the root-mean-square radius of the proton charge distribution is equal to $\sqrt{0.69} = 0.83$ fm.

[5]In [10], $\rho_0 = 0.157$ fm^{-3} is used for ^{208}Pb (to be compared to the standard 0.17).

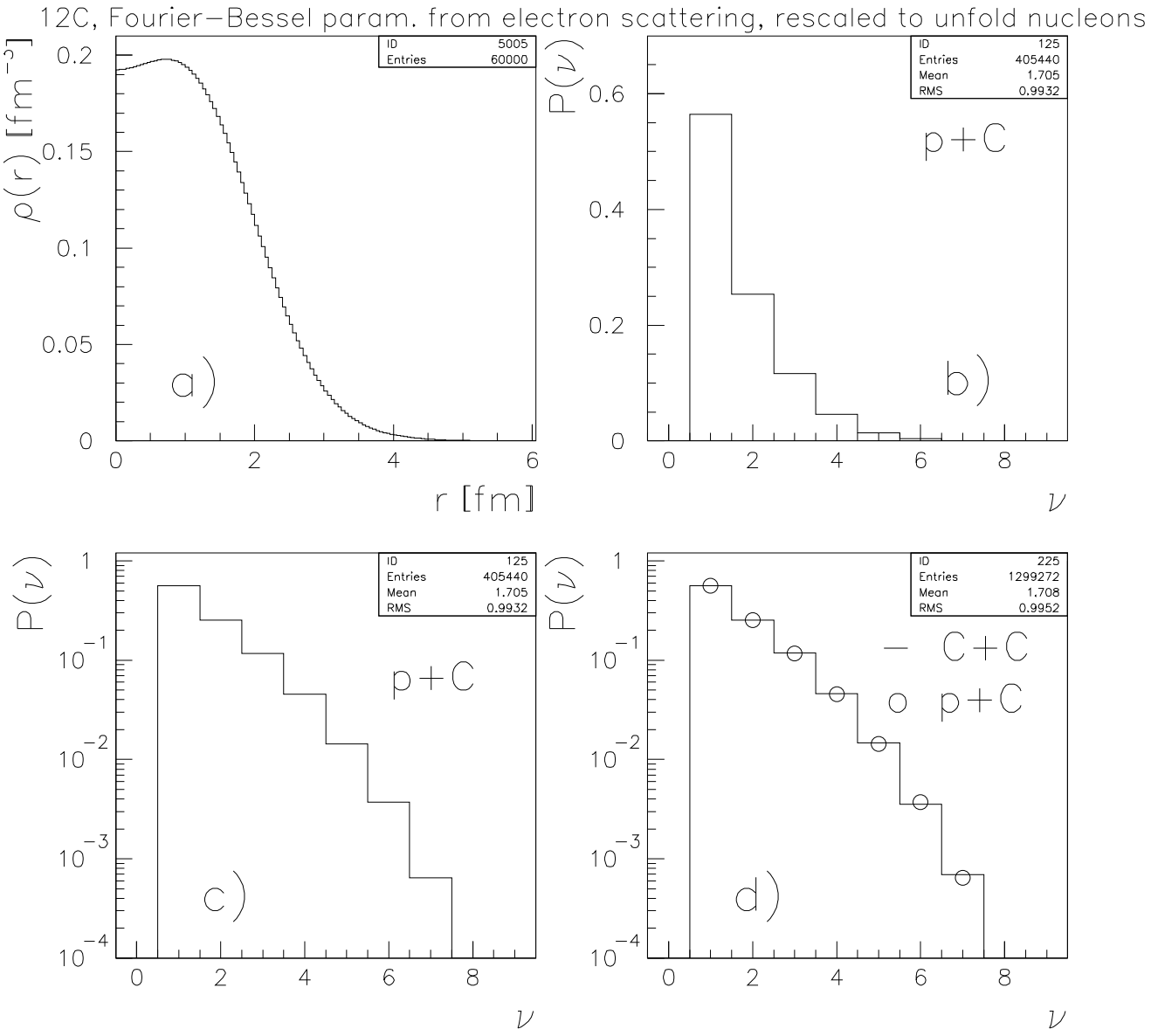

Figure 12: Results of the simulation assuming $\rho(r)$ as obtained from prescription (2) on the basis of the Fourier-Bessel charge distributions [13]. a) absolutely normalized nucleon density profile, b) resulting probability distribution of $< \nu >$ in proton+carbon reactions, c) same on a log scale, d) $< \nu >$ distribution per participant in C+C reactions (histogram with displayed corresponding statistical parameters) compared to that in p+C reactions (circles).

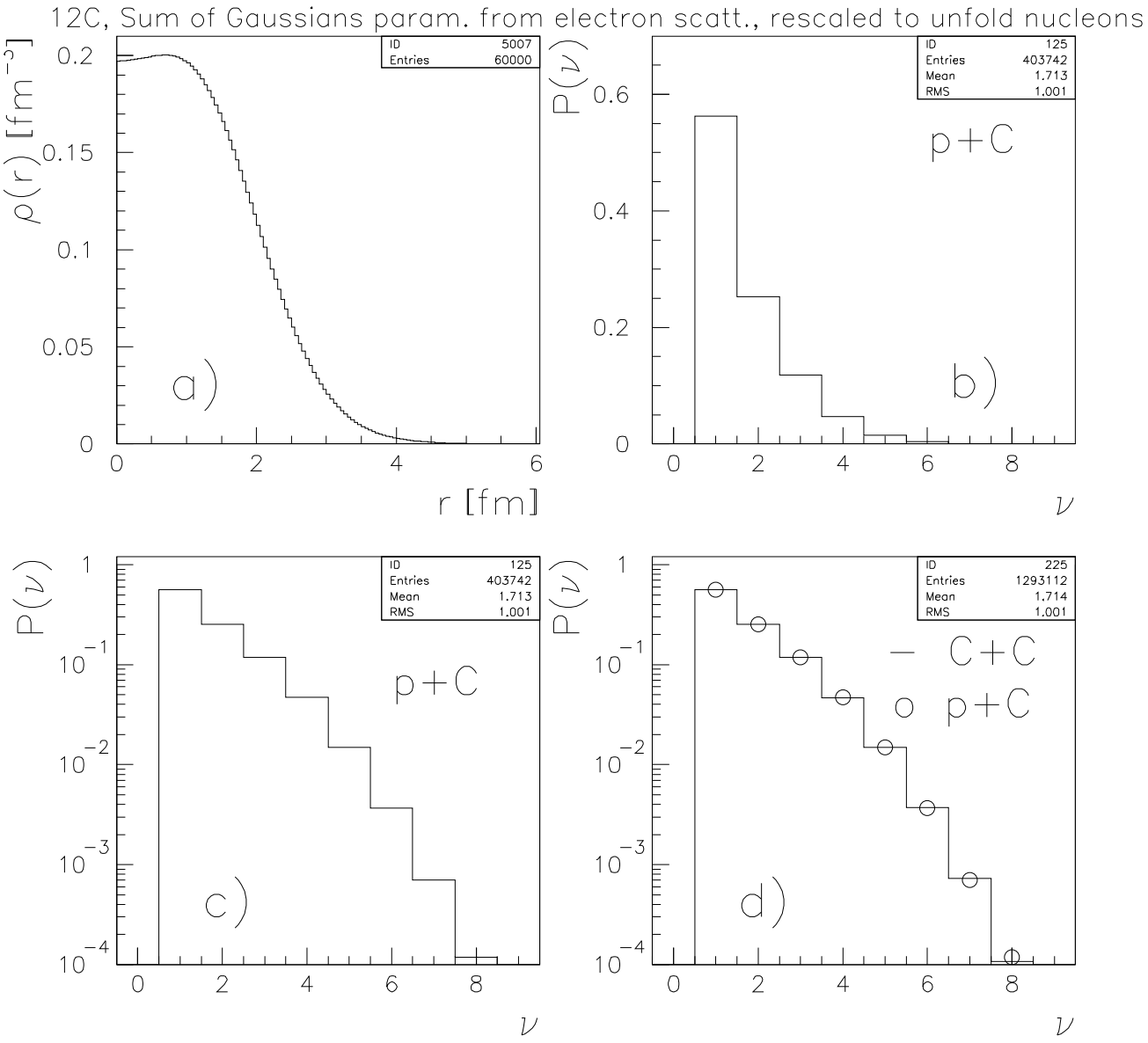

Figure 13: Results of the simulation assuming $\rho(r)$ as obtained from prescription (2) on the basis of the Sum-of-Gaussians charge distributions [14]. a) absolutely normalized nucleon density profile, b) resulting probability distribution of $< \nu >$ in proton+carbon reactions, c) same on a log scale, d) $< \nu >$ distribution per participant in C+C reactions (histogram with displayed corresponding statistical parameters) compared to that in p+C reactions (circles).

of participant pairs is 3.60 ± 0.01 while the $< \nu >$ value is 1.714 ± 0.002. Relative to the non-unfolded spectra discussed in Sec. 5.2, this represents a change of respectively +0.075 collisions, -11 mb, +0.15 participant pairs, +0.075 collisions, almost identically to the Fourier-Bessel case from Sec. 6.1.

For reference the numerical values of probabilities $P(\nu)$ are given below:

```
 12C, Sum of Gaussians param. from electron scatt., rescaled to unfold
 nucleons
              p+C      C+C
 P(1)   =   0.5628   0.5619
 P(2)   =   0.2527   0.2538
 P(3)   =   0.1179   0.1180
 P(4)   =   0.0471   0.0468
 P(5)   =   0.0149   0.0149
 P(6)   =   0.0037   0.0037
 P(7)   =   0.0007   0.0007
 P(8)   =   0.0001   0.0001
```

7 Additional Details of Secondary Importance

For completeness, a description of the influence of the exact value of the elementary cross-section and of the way in which statistical errors have been treated is included below.

7.1 Elementary Cross-Section

The elementary nucleon-nucleon cross-section used in the geometrical model (Sec. 3) is known to some accuracy. This has been tentatively assumed to be given by the difference between its NA49 value determined in [6] and the literature value of 31.78 mb quoted therein. In order to verify the influence of such a change of cross-section on the determination of centrality parameters discussed here, an additional study has been made. For this study, the elementary cross-section has been assumed equal to 31.78 mb, while the nuclear density profile has been kept identical to that discussed in Sec. 6.2.

Assuming this, one gets the **results** presented in Fig. 14. For minimum bias p+C reactions the obtained $< \nu >$ value is 1.720 ± 0.002. The p+C inelastic cross-section is predicted to be 222 ± 0.6 mb. For C+C reactions the predicted mean number of participant pairs is 3.61 ± 0.01 while the $< \nu >$ value is 1.722 ± 0.002. Relative to the standard elementary cross-section of 31.42 mb used in the whole study, the same nuclear density profile (Sec. 6.2) gives a change of respectively +0.007 collisions, +2 mb, +0.01 participant pairs, +0.008 collisions.

For reference the numerical values of probabilities $P(\nu)$ are given below:

```
 12C, Sum of Gaussians param. from elect.scatt.,rescaled,
sigmainel(pp)=31.78 mb
              p+C      C+C
 P(1)   =   0.5602   0.5592
 P(2)   =   0.2533   0.2536
 P(3)   =   0.1187   0.1192
 P(4)   =   0.0473   0.0476
 P(5)   =   0.0157   0.0155
 P(6)   =   0.0038   0.0039
 P(7)   =   0.0008   0.0008
 P(8)   =   0.0001   0.0001
```

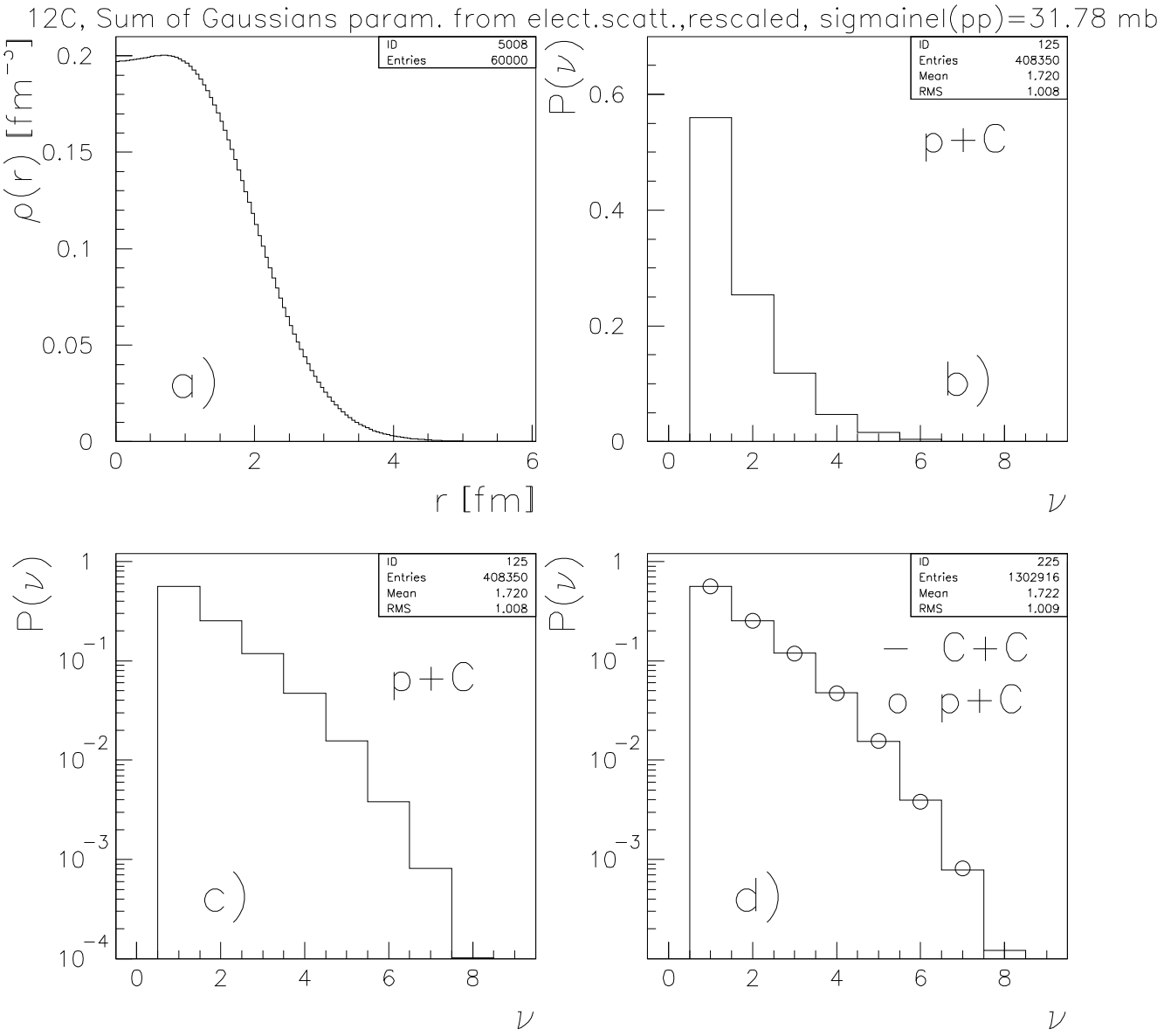

Figure 14: Results of the simulation assuming $\rho(r)$ as obtained from prescription (2) on the basis of the Sum-of-Gaussians charge distribution [14], *with the assumption of the elementary nucleon-nucleon cross-section being equal to 31.78 mb.* a) absolutely normalized nucleon density profile, b) resulting probability distribution of $< \nu >$ in proton+carbon reactions, c) same on a log scale, d) $< \nu >$ distribution per participant in C+C reactions (histogram with displayed corresponding statistical parameters) compared to that in p+C reactions (circles).

7.2 Statistical Studies

As the distributions of ν and of the number of participants differ very much from Gaussians, it was not clear whether the error of their mean could be defined as $\frac{r.m.s.}{\sqrt{N(entries)}}$.

To check this, the total Monte-Carlo sample used for studies of rescaled Sum-of-Gaussian nuclear profiles (similar[6] to that in Sec. 6.2) has been divided into 16 independent sub-samples and the resulting distributions of all the considered centrality parameters have been plotted in Fig. 15. Realistic standard deviations have been deduced from hand-made Gaussian fits shown in the Figure. On that basis, formulae for statistical errors have been deduced. In case of discrepancies between the mean obtained from the fit and that obtained from the total sample, the error has been enlarged to take the uncertainty of the hand-made fit into account. The resulting formulae are:

a) for the mean number of elementary collisions in p+C:
absolute error = $1.33\ \frac{r.m.s.}{\sqrt{N(entries)}}$.

b) for the p+C inelastic cross-section:
relative error = $\frac{0.856}{\sqrt{N(entries)}}$.

c) for the mean number of participants in C+C:
absolute error = $\frac{4.3}{\sqrt{N(entries)}}$.

d) for the mean number of elementary collisions in C+C:
absolute error = $1.8\ \frac{r.m.s.}{\sqrt{N(entries)}}$.

The $r.m.s.$ and $N(entries)$ are always taken from the corresponding distributions in Figs 3-14. Note that for d), $N(entries)$ does not correspond to the number of generated minimum-bias events but to the total number of generated participating nucleons.

8 Summary of Results and Proposed Final Estimates

A summary of all the results presented in this Chapter is shown in Table 1. For establishing the final, best estimates for the centrality parameters considered here, the following reasoning is applied:

- The final **values** of all the centrality parameters are assumed to be the ones obtained from the Fourier-Bessel and Sum-of-Gaussians nuclear density profiles after the primitive unfolding method from Sec. 6 has been applied. This is consistent with the general approach of the model which deals with the respective geometrical position of the nucleon's "center of gravity". While some doubts have arisen in Sec. 6 (Fig. 11) about the apparently high value of the unfolded $\rho(r)$ reaching up to 0.2 fm^{-3} for small r values, it is unlikely that that would be an artifact of the unfolding method. Finally, as the values of $< r^2 >^{\frac{1}{2}}$ are anyway directly fixed by eq. (1), the mere deviation of the shape of the density profile from reality should not result in large changes of centrality parameters. This is apparent in the small difference between Saxon-Woods and Gaussian parametrizations shown in Table 1.
- As there is no reason to favour the Fourier-Bessel or the Sum-of-Gaussians parametrization, the mean of the corresponding centrality parameters has been taken for the final estimate.
- To establish a realistic estimate of the corresponding **error bars** is much less trivial. Finally the applied error bar has been set as a *linear* sum of two components:

[6]The statistical study made here corresponds to an earlier version of the rescaled Sum-of-Gaussian study, assuming by mistake $< r^2_{proton\ charge} >= 0.33$ instead of 0.69 fm^2. This mistake has been corrected for the analysis made in Sec. 6.2, but there was no sense to repeat the statistical study made here.

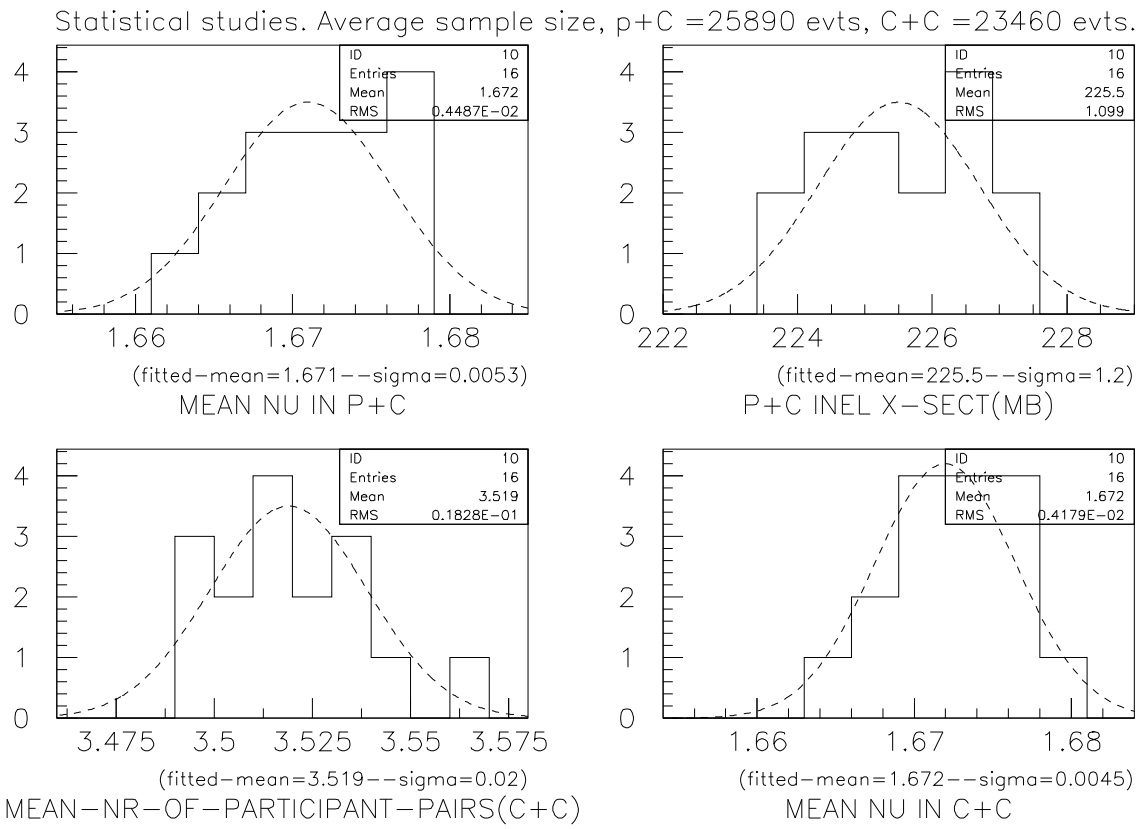

Figure 15: Results of statistical studies of the centrality parameters. Distributions of $< \nu >$ in p+C collisions (upper left), of the p+C inelastic cross-section (upper right), of the mean number of participants (lower left) and of $< \nu >$ in C+C collisions (lower right), as obtained from a subdivision of the total Monte-Carlo sample into 16 independent sub-samples.

	method (nuclear profile)	elementary cross-section [mb]	$< r^2 >^{\frac{1}{2}}$ [fm]	p+C $< \nu >$	p+C cross-section [mb]	C+C number of participant pairs	C+C $< \nu >$
simple--minded (Sec. 4)	Saxon-Woods	31.42	2.778	1.520 ± 0.004	248 ± 1	3.15 ± 0.02	1.516 ± 0.003
	Gaussian	31.42	2.778	1.516 ± 0.004	249 ± 1	3.14 ± 0.02	1.519 ± 0.003
	Sharp Sphere	31.42	1.986	1.941 ± 0.006	196 ± 1	4.10 ± 0.02	1.933 ± 0.004
charge distrib. (Sec. 5)	Fourier-Bessel	31.42	2.478	1.631 ± 0.002	231 ± 0.5	3.45 ± 0.01	1.634 ± 0.002
	Sum-of-Gaussians	31.42	2.469	1.638 ± 0.002	231 ± 0.5	3.45 ± 0.01	1.639 ± 0.002
rescaled charge distrib. (Sec. 6)	Fourier-Bessel	31.42	2.334	1.705 ± 0.002	221 ± 0.5	3.59 ± 0.01	1.708 ± 0.002
	Sum-of-Gaussians	31.42	2.325	1.713 ± 0.002	220 ± 0.5	3.60 ± 0.01	1.714 ± 0.002
x-check (Sec. 7)	Sum-of-Gaussians	31.78	2.325	1.720 ± 0.002	222 ± 0.6	3.61 ± 0.01	1.722 ± 0.002
	proposed estimate	**31.42 ± 0.36**	**2.330 ± 0.005**	**1.71 ± 0.05**	**220 ± 8**	**3.60 ± 0.09**	**1.71 ± 0.05**

Table 1: Compendium of results of all the simulations presented in this Chapter, together with proposed estimates for final centrality parameters. For simulation results error bars are purely statistical; error bars on the proposed estimates are established as discussed in the text.

(a) half of the difference between the value of a given centrality parameter for the nucleon unfolded case (Sec. 6) and the value for the non-unfolded case (Sec. 5); this assumes that the change of nucleon densities obtained from the unfolding procedure (Fig. 11) may be wrong by a factor of two[7].

(b) the difference between the value of a given centrality parameter assuming the elementary cross-section equal to 31.78 mb and the corresponding value assuming the standard 31.42 mb (see Sec. 7.1.).

- Other error sources, and specifically the relatively small statistical errors, are neglected.

As it was pointed out in Sec. 4, the $< \nu >$ values appear to be the same (1.71 ± 0.05) in minimum bias p+C and C+C reactions; a comment will be made in the Sec. 9.

For completeness, an estimate for the probability distribution of the number of collisions in minimum bias p+C reactions is given below. It is obtained as the average of $P(\nu)$ distribution obtained on the basis of rescaled Fourier-Bessel and Sum-of-Gaussian density profiles. Similarly to the mean value $< \nu >$, also the distribution should be the same in p+C and C+C reactions.

```
 12C, Average of probability distributions P(nu) obtained from
rescaled Fourier-Bessel and Sum-of-Gaussians parametrizations.
              p+C
 P(1)   =   0.5637
 P(2)   =   0.2534
 P(3)   =   0.1173
 P(4)   =   0.0464
 P(5)   =   0.0147
 P(6)   =   0.0037
 P(7)   =   0.0006
 P(8)   =   0.0001
```

9 Discussion of Further Problems

The following items are to be considered in any further continuation of the work presented in this Chapter.

1. Unfolding of charge distributions could surely be made in a more precise way relative to the primitive approach presented here, either by precise methods like Fourier transforms [7], or by simple numerical adjustment methods. More knowledge on the shape of the proton charge distribution will have to be gathered. Some discussion of the subject can be still found in [10].
2. According to [7, 8], for isospin-symmetric nuclei the neutron root-mean-square radius might be *smaller* than the proton root-mean-square radius. This is opposite to the situation known from ^{208}Pb, and would imply a slightly denser carbon nucleus relative to the one assumed here. In principle one would expect only a small effect.
3. Account taken of the missing information on neutrons, a serious nuclear physics model calculation would be useful if more understanding on the whole subject is to be gathered. Such a calculation could be cross-checked by means of antiprotonic atom data on other nuclei [8].

[7] One may get an idea of the corresponding uncertainties by considering eqs. (1-2). A change by a factor of two would imply, for instance, the root-mean-square radius of the proton charge distribution being equal to 0.6 fm instead of 0.83 fm, corresponding to maximal values of $\rho(r) \approx 0.18$-0.185 instead of 0.2 fm^{-3}.

Two final remarks are to be included.

- The strict similarity of $< \nu >$ values and $P(\nu)$ distributions in minimum bias p+C and C+C reactions seems to be an inherent feature of the geometrical approach considered here. Indeed, considering a uniform flux of C nuclei impinging on a C target, each of the projectile participants scans the target nucleus in an unbiased way, just as in p+C collisions.
- The standard relation

$$< \nu >= A\frac{\sigma_{pp}}{\sigma_{pA}} \tag{3}$$

is also a general, inherent feature of the geometrical approach discussed here. As such, the value of $< \nu >$ coming from the above ratio of experimentally known inelastic cross-sections should be correct, even if the nuclear density profile is not known (see also the discussion made in [5]). That means that the result of any correct model calculation should agree with the value $< \nu >= 1.68$ quoted in [5, 17], within the error bars corresponding to that value. The present study gives $< \nu >= 1.71 \pm 0.05$, which suggests a reasonable agreement between the two values. Further comparisons between geometrical model predictions and values deduced directly from experimental data will be made in the subsequent Chapter.

Part II
Contribution of Single Collisions to Minimum Bias Hadron-Carbon and Hadron-Lead Reactions

10 Motivation

The centrality analysis described in Part I has been subsequently extended to other hadron-nucleus reactions. The goal for the study presented below was to estimate and compare the values of $< \nu >$, of the total inelastic cross-section, and finally of the fraction of single collisions $P(1)$ for the following reactions: p+C, π^++C, π^-+C, p+Pb, π^++Pb, π^-+Pb. The study was made by means of the same geometrical model as described in Sec. 3.

The motivation for this study was:

1. to get an idea on the dependence of the hadron-nucleus centrality parameters on hadron type and nucleus size;
2. to verify, by comparison of the predicted and measured inelastic cross-section, to what extent the simple geometrical model used here describes reality;
3. to allow for the extraction of the non-elementary component of hadron-nucleus reactions. This operation is described in detail in [5]; it obviously requires a reasonably precise knowledge of the relative contribution $P(1)$ of single hadron-nucleon events in a minimum bias hadron-nucleus sample.

The remainder of this Chapter contains a discussion of assumed input elementary cross-sections and nuclear profiles, a description of the way in which the various uncertainties have been estimated, and a table of final estimates on centrality parameters compared to measured inelastic cross-sections. A discussion of these results is also included.

11 Input Values, Uncertainties and the Way They Have Been Estimated

The following uncertainty sources were taken into account:

11.1 Uncertainty of the Elementary Cross-section

As described in Sec. 7.1, the elementary hadron-nucleon cross-sections are known to a given accuracy. Similarly to what has been done in the precedent Chapter, the following assumptions have been made for the present analysis:

- σ_{p+p}: the value of 31.42 mb has been assumed (see discussion made in Sec. 3). An uncertainty of about 1% has been postulated on the basis of the difference between NA49 data and literature [6].
- $\sigma_{\pi^+ + p}$: the value of 20.35 mb has been assumed, based on [18]. An uncertainty of 1% has been postulated.
- $\sigma_{\pi^- + p}$: the value of 20.80 mb has been assumed, based on [18]. An uncertainty of 1% has been postulated.

As the π^++p and π^-+p cross-sections differ by 2.2%, a 1% uncertainty allows for these two cross-sections to be equal which could be expected on the basis of various arguments [4]. It is worthwhile to mention that isospin effects [19] have not been considered in the elementary cross-section assumed in the model: for all the studies described in the present and subsequent Chapter all the p+p, p+n, n+p, n+n collisions taking place in p+Pb and Pb+Pb reactions have been assumed to have the p+p cross-section; all the π^++p and π^++n collisions taking place in π^++Pb reactions have been assumed to have the π^++p cross-section; analogically for π^-+Pb reactions.

11.2 Uncertainty of the Target Nuclear Profile

As it has been demonstrated in the previous Chapter, the centrality parameters in minimum bias hadron-nucleus reactions depend on the density profile assumed for the target nucleus. This introduces an uncertainty which has to be evaluated.

For the C target, this uncertainty has been estimated by applying two different charge profiles (Fourier-Bessel, Sum-of-Gaussians), rescaled linearly to unfold nucleon distributions (see detailed discussion in Sec. 6). The quoted error includes the unfolding uncertainty discussed in Sec. 8. For π^++C and π^-+C reactions, the relative error from unfolding has been assumed to be equal to that estimated for p+C collisions.

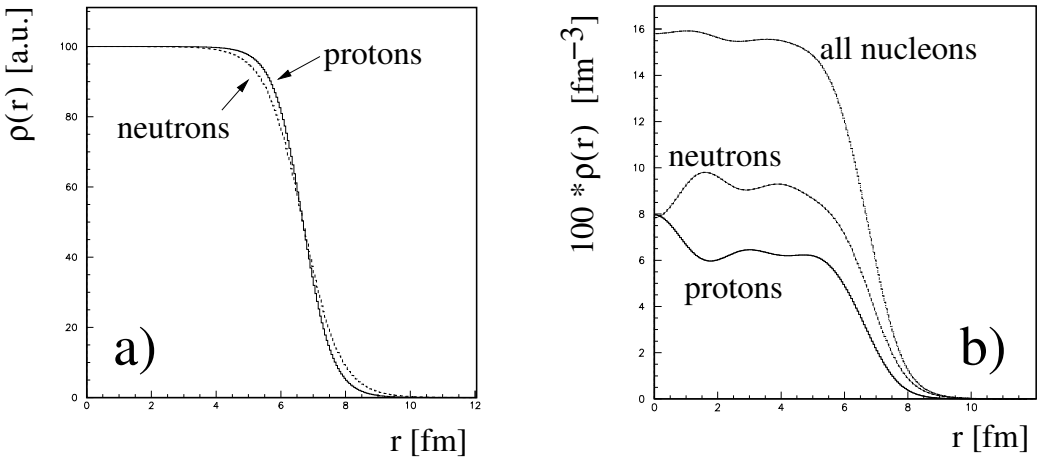

Figure 16: The two sets of proton and neutron density profiles used for the ^{208}Pb nucleus: **a)** the data parametrizations [10], *arbitrarily normalized* to the common value of 100 at $r = 0$, and **b)** the profiles obtained from the Hartree-Fock-Bogoliubov calculation [20], absolutely normalized.

For the Pb target, the uncertainty has been estimated by applying two different sets of proton and neutron density profiles available for ^{208}Pb. The first set [10] gives the proton and neutron profiles in terms of analytical Saxon-Woods parametrizations (Sec. 4.1); it is based, among others, on antiprotonic atom data. The second set is a result of a Hartree-Fock-Bogoliubov theoretical calculation [20]. Both considered sets are shown in Fig. 16. Account taken of the fact that the first set (panel **a**) is shown in an arbitrary normalization to the same value for protons and neutrons, while the second set (panel **b**) is shown in an absolute scale, one notes that they differ very significantly as far as the postulated neutron over proton ratio at $r = 0$ is concerned.

11.3 Uncertainty Induced by the Natural Pb Target

The present study being made in order to provide a background for the analysis and interpretation of NA49 experimental data, an additional uncertainty has to be taken into account. As discussed in [21], the NA49 lead target is not made of pure ^{208}Pb isotope. It is in fact a "natural target" with an average $A = 207.2$. This might induce a possible effect on both p+Pb and Pb+Pb reactions (note that the NA49 Pb beam exclusively consists of ^{208}Pb ions).

This uncertainty is estimated by assuming the natural target to be composed of ^{207}Pb (80%) and ^{208}Pb (20%). As to the best of author's knowledge, no proton and neutron nuclear profiles of the type used for ^{208}Pb are available for ^{207}Pb, the difference between ^{207}Pb and ^{208}Pb is estimated by assuming, for ^{207}Pb, the ^{208}Pb nuclear profile [10] extrapolated down to $A = 207$ by means of the general $R \sim A^{\frac{1}{3}}$ empirical parametrization (Sec. 4.1). As such, the proton and neutron half-density radii are both scaled down by $(207/208)^{\frac{1}{3}}$ while the surface thickness parameters remain unchanged. The simulation is then made for both hadron-^{207}Pb and hadron-^{208}Pb minimum bias reactions; for each of the considered centrality parameters, the final obtained value is constructed as a weighted average:

$$\text{hadron-(natural target)} = 80\% \cdot (\text{hadron-}^{207}\text{Pb}) + 20\% \cdot (\text{hadron-}^{208}\text{Pb})$$

12 Results

In order to take account of all the uncertainties discussed in the precedent Section, numerous simulations have been performed with different input parameters (elementary cross-sections, nuclear profiles, etc). On the basis of these simulations, and following an approach similar to that proposed in Sec. 8, final estimates for $< \nu >$, the inelastic hadron-nucleus cross-section, and $P(1)$ have been obtained for each of the considered reactions. Corresponding error bar estimates have been elaborated; these take account of all the error sources quoted above. They also include the statistical errors of the Monte-Carlo.

Table 2 displays all these final estimates; these Monte-Carlo results are then compared to the measured values of the inelastic hadron-nucleus cross-section and to the corresponding mean number of elementary collisions deduced from the standard relation (3).

13 Comments

1. The difference between the error bars for the C target (relative error 3-4%) and the Pb target (relative error 1-2%) comes from the large uncertainty attributed to the primitive nucleon unfolding procedure discussed in Secs 6 and 8. Thus for p+C and π+C reactions there is still some room for decreasing these uncertainties once a more precise method is elaborated. This is not the case for p+Pb and π+Pb interactions as here nucleon densities have been directly available.
2. The relative deviation between the Monte-Carlo values and corresponding measured quantities does not exceed 3% for hadron-carbon collisions which is within both Monte-Carlo and experimental errors[8]. For hadron-lead collisions the deviations are bigger, although they do not exceed 6%. This difference between the C and Pb target seems quite surprising in view of the fact that for hadron-carbon collisions, the method to obtain the nucleon profile from charge distributions (Sec. 6) is in principle more primitive and less precise relative to what is available for hadron-lead reactions.

[8]Note: a 2.5% systematic error on the inelastic p+C cross-section is quoted in [17].

reaction		$< \nu >$	inelastic cross-section [mb]	$P(1)$
p+C	Monte-Carlo experiment [5, 17] deviation MC/exp	1.71 ± 0.05 1.68 +1.8%	220 ± 8 226 -2.7%	0.563 ± 0.018
π^++C	Monte-Carlo experiment [18] deviation MC/exp	1.47 ± 0.04 1.43 +2.8%	166 ± 6 171 -2.9%	0.664 ± 0.021
π^-+C	Monte-Carlo experiment [18] deviation MC/exp	1.48 ± 0.04 1.47 +0.7%	169 ± 6 170 -0.6%	0.659 ± 0.021
p+Pb	Monte-Carlo experiment [22] deviation MC/exp	3.75 ± 0.05 3.61 +3.9%	1736 ± 17 1806 ± 25 -3.9%	0.232 ± 0.004
π^++Pb	Monte-Carlo experiment [18] deviation MC/exp	2.76 ± 0.04 2.85 -3.2%	1528 ± 16 1485 +2.9%	0.308 ± 0.005
π^-+Pb	Monte-Carlo experiment [18] deviation MC/exp	2.79 ± 0.04 2.95 -5.4%	1542 ± 16 1467 +5.1%	0.304 ± 0.005

Table 2: Compendium of final estimates on centrality parameters: $< \nu >$, the inelastic hadron-nucleus cross-section, and $P(1)$ as coming from the Monte-Carlo calculation, together with corresponding experimental values. The relative deviation between Monte-Carlo and experiment is also indicated.

3. Finally, it is to be mentioned that $P(1)$ appears as a robust result of the Monte-Carlo. This, taken together with the reasonable agreement of the geometrical approach presented here with the experimental data (especially for C targets) gives confidence in the estimates obtained for $P(1)$.

Part III
Centrality Dependence of Pb+Pb and p+Pb Interactions

14 Motivation

This Chapter summarizes the analysis of the impact parameter dependence of various quantities characterizing the Pb+Pb and p+Pb reaction. The two main motivations for performing this study were:

1. To get an idea on the evolution of various parameters defining centrality, account taken of realistically estimated uncertainties induced by the nuclear profile and by the limited precision to which the elementary cross-section is known. This motivation mostly concerns the probability $P(\nu)$ for the participant nucleon to hit a given number ν of nucleons belonging to the other nucleus, and most of all the single collision contribution $P(1)$. Similarly to what is done for p+C collisions [5], this quantity may be used to extract the non-elementary component of centrality-selected Pb+Pb and p+Pb reactions.

   Additionally, other useful centrality parameters - the mean number of participating nucleons, the mean number $< \nu >$ of elementary collisions - have also been studied as function of the impact parameter of the reaction.

2. To get a realistic estimate on the influence of the neutron halo (or: of the difference between the proton and neutron density profiles in the Pb nucleus) on the relative abundance of protons and neutrons participating to the reaction. As the proton/neutron content of the nucleus influences particle production at high energies [19], quantitative knowledge of this problem is necessary for the interpretation of phenomena taking place in heavy ion reactions at the SPS.

   This part of the analysis was essentially similar to that published in [23], the principal difference being that it did not rely on model-dependent particle production mechanisms. Instead, the impact parameter dependence of the participating neutron/proton ratio was directly studied. As argued in [5, 19], this quantity is by itself convenient to construct predictions for particle production in nuclear reactions.

The analysis was performed using the same model as defined in Sec. 3. The only difference was that instead of a uniform flux of projectiles used for minimum bias reactions, the present simulation assumed lead nuclei (or proton projectiles) always positioned at a given impact parameter relative to the Pb target. In addition to various quantities discussed in the preceding Chapters, the simulation recorded the number of participating protons and neutrons in view of item. 2.

15 Uncertainties & Conventions

An important goal of the present study was to get an idea on the size of uncertainties induced by the elementary cross-section (see Sec. 11.1), by the Pb nuclear profile (Sec. 11.2) and by the problem of the NA49 natural Pb target (Sec. 11.3). In view of these, all the simulations of Pb+Pb reactions have been made in four different options:

1) simulation of a ^{208}Pb+^{208}Pb collision. The elementary cross-section has been assumed to be 31.42 mb (see precedent Chapters for discussion). For each of the two nuclei, the nuclear profile coming from the parametrization [10] (Fig. 16a) has been assumed. In

various Figures discussed below, this nuclear profile is labeled "AT", while the result of this simulation is drawn by means of **full dots**.

2) simulation of a ^{207}Pb+^{207}Pb collision. The elementary cross-section has been assumed to be 31.42 mb. For each of the two nuclei, the nuclear profile coming from the parametrization [10] has been extrapolated down to $A = 207$ in the way specified in Sec. 11.3. In the Figures discussed below, this nuclear profile is labeled "AT-extrapolated ", while the result of this simulation is drawn by means of **solid curves**.

3) simulation of a ^{208}Pb+^{208}Pb collision. The elementary cross-section has been assumed to be 31.42 mb. For each of the two nuclei, the nuclear profile coming from the Hartree-Fock-Bogoliubov calculation [20] (Fig. 16b) has been assumed. In the Figures discussed below, this nuclear profile is labeled "HFB", while the result of this simulation is drawn by means of **open squares**.

4) simulation of a ^{208}Pb+^{208}Pb collision. The elementary cross-section has been assumed to be 31.78 mb (see Secs 7.1 and 11.1 for discussion). For each of the two nuclei, the nuclear profile coming from the parametrization [10] has been assumed as in option **1)**. In Figures discussed below, this nuclear profile is again labeled "AT" and the cross-section modification is indicated by the label "modified el.x-section". The result of this simulation is drawn by means of **open circles**.

This approach allows for an immediate identification of the importance of the various error sources discussed. For instance, the difference between options **1)** and **2)** gives an idea of the uncertainties induced by the natural Pb target. The difference between options **1)** and **3)** displays the influence of the nuclear profile, while the difference between options **1)** and **4)** shows the uncertainty induced by the elementary cross-section. The comparison of the four options taken together gives then an idea of the resulting total error.

For p+Pb interactions a strictly similar approach has been followed, with p+^{208}Pb reactions (options **1**, **3**, **4**) and p+^{207}Pb reactions (option **2**) being respectively simulated with different elementary cross-sections and different nuclear density profiles.

16 The Dependence of $P(\nu = 1, 2...)$ on Impact Parameter

The discussion of the obtained results begins with the dependence of the probabilities $P(1)$, $P(2)$, and further, on impact parameter b. Fig. 17 displays this dependence for the Pb+Pb reaction; the same plot is magnified in Fig. 18.

As seen in the two plots, the differences between the four options considered in the precedent Section are small, of the order of 0.01 or less. The fraction of single collisions $P(1)$ appears to follow a monotonic decrease from 90% at $b = 17$ fm down to 8.5% at $b = 0$ fm.

For comparison, Figs 19 and 20 display the same $P(\nu)$ dependence on b for p+Pb reactions. Trivially, all the apparent trends are compressed towards lower b values and the corresponding structures are sharper.

To complete the picture, examples of $P(\nu)$ distributions at fixed impact parameter values are shown in Fig. 21 and Fig. 22 for Pb+Pb and p+Pb reactions, respectively. The displayed distributions correspond to simulations made assuming the elementary cross section of 31.42 mb, the "AT" nuclear profile, and the ^{208}Pb nucleus (option **1** from the precedent Section). It is to be noted that typical ν values reached in central Pb+Pb reactions, at $b = 0$ (Fig. 21) are significantly lower relative to these reached in p+Pb interactions at $b = 0$ (Fig. 22). Also, the elementary contribution $P(1)$ appears much larger in central Pb+Pb relative to p+Pb reactions. This simple geometrical effect of higher effective centrality in selected samples of p+Pb collisions is known to bring consequences for observed phenomena like baryon stopping (see discussion made in [24]).

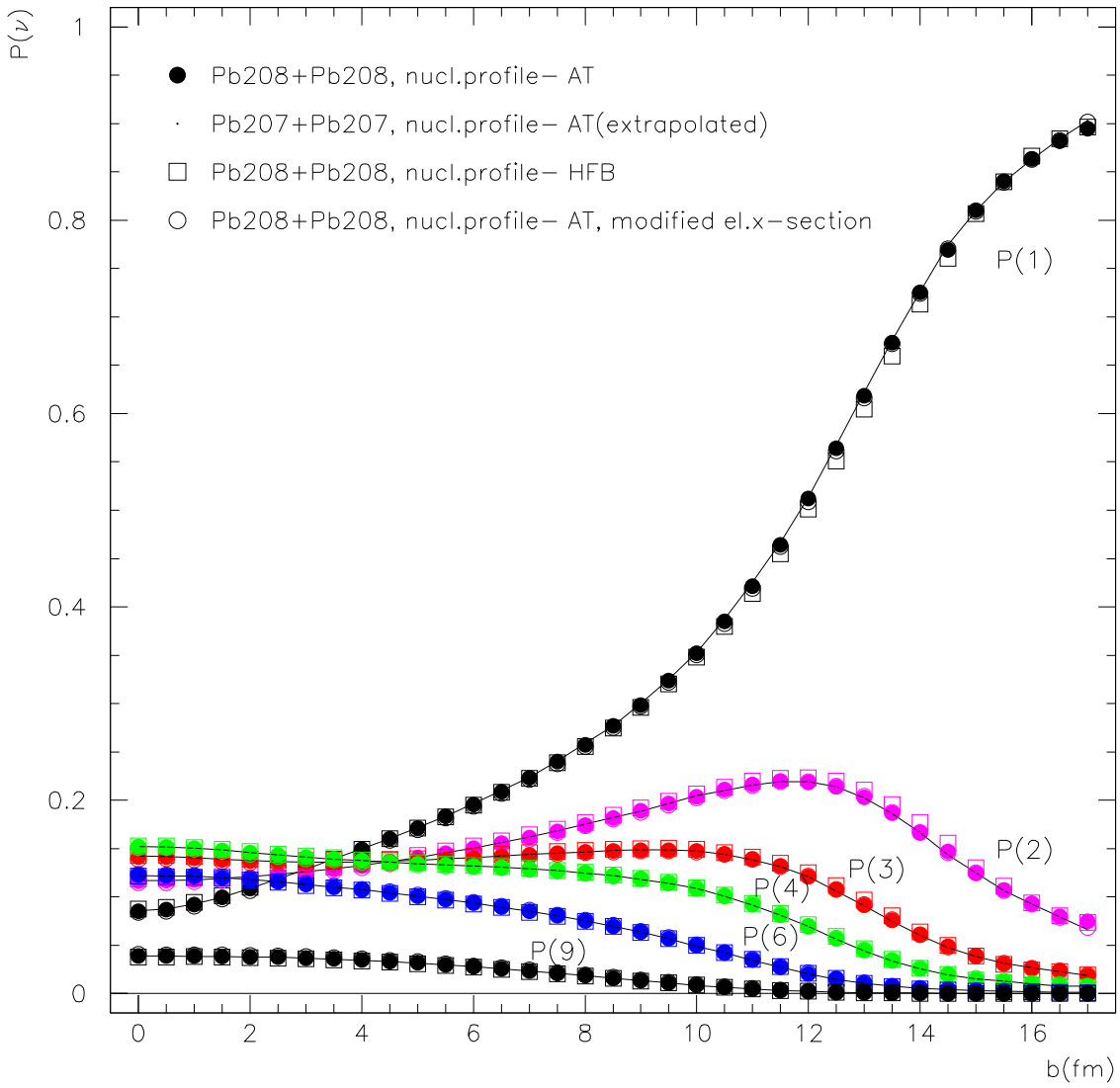

Figure 17: Impact parameter dependence of probabilities $P(1)$, $P(2)$, $P(3)$, $P(4)$, $P(6)$, and $P(9)$ for the Pb+Pb reaction. The four Monte-Carlo options discussed in Sec. 15 are displayed by means of different symbols.

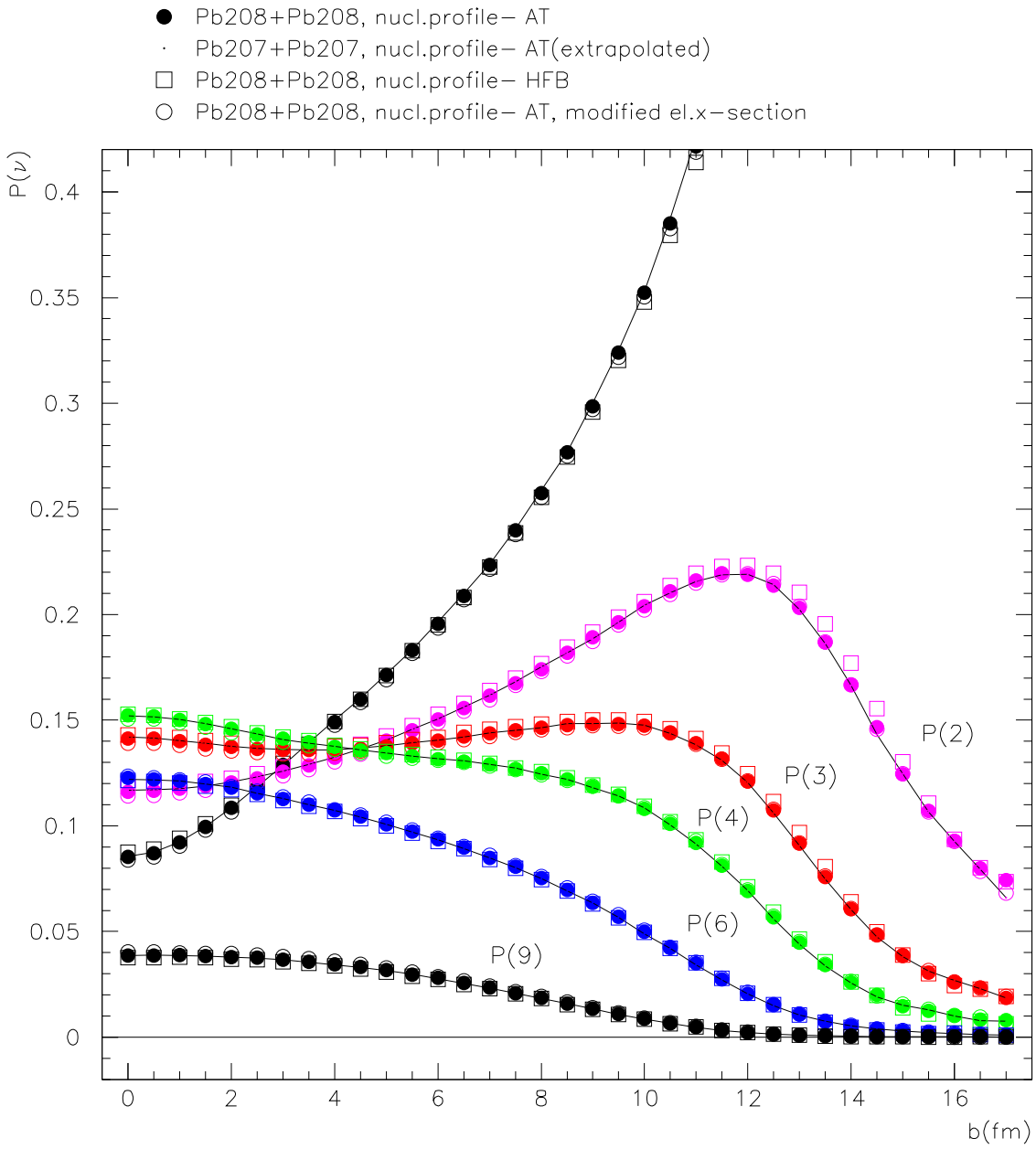

Figure 18: Impact parameter dependence of probabilities $P(1)$, $P(2)$, $P(3)$, $P(4)$, $P(6)$, and $P(9)$ for the Pb+Pb reaction *(magnified plot)*. The four Monte-Carlo options discussed in Sec. 15 are displayed by means of different symbols.

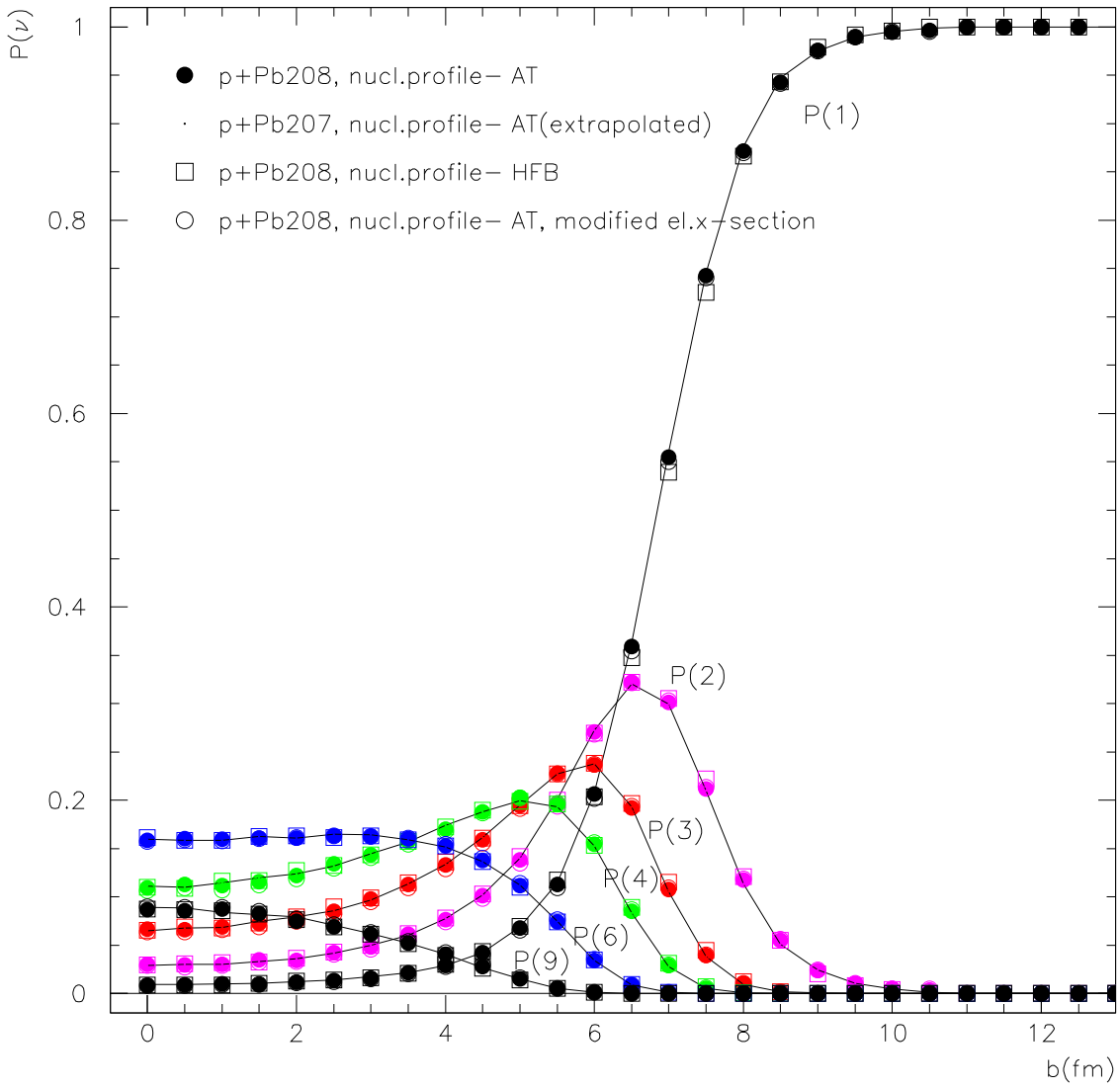

Figure 19: Impact parameter dependence of probabilities $P(1)$, $P(2)$, $P(3)$, $P(4)$, $P(6)$, and $P(9)$ for the p+Pb reaction. The four Monte-Carlo options discussed in Sec. 15 are displayed by means of different symbols.

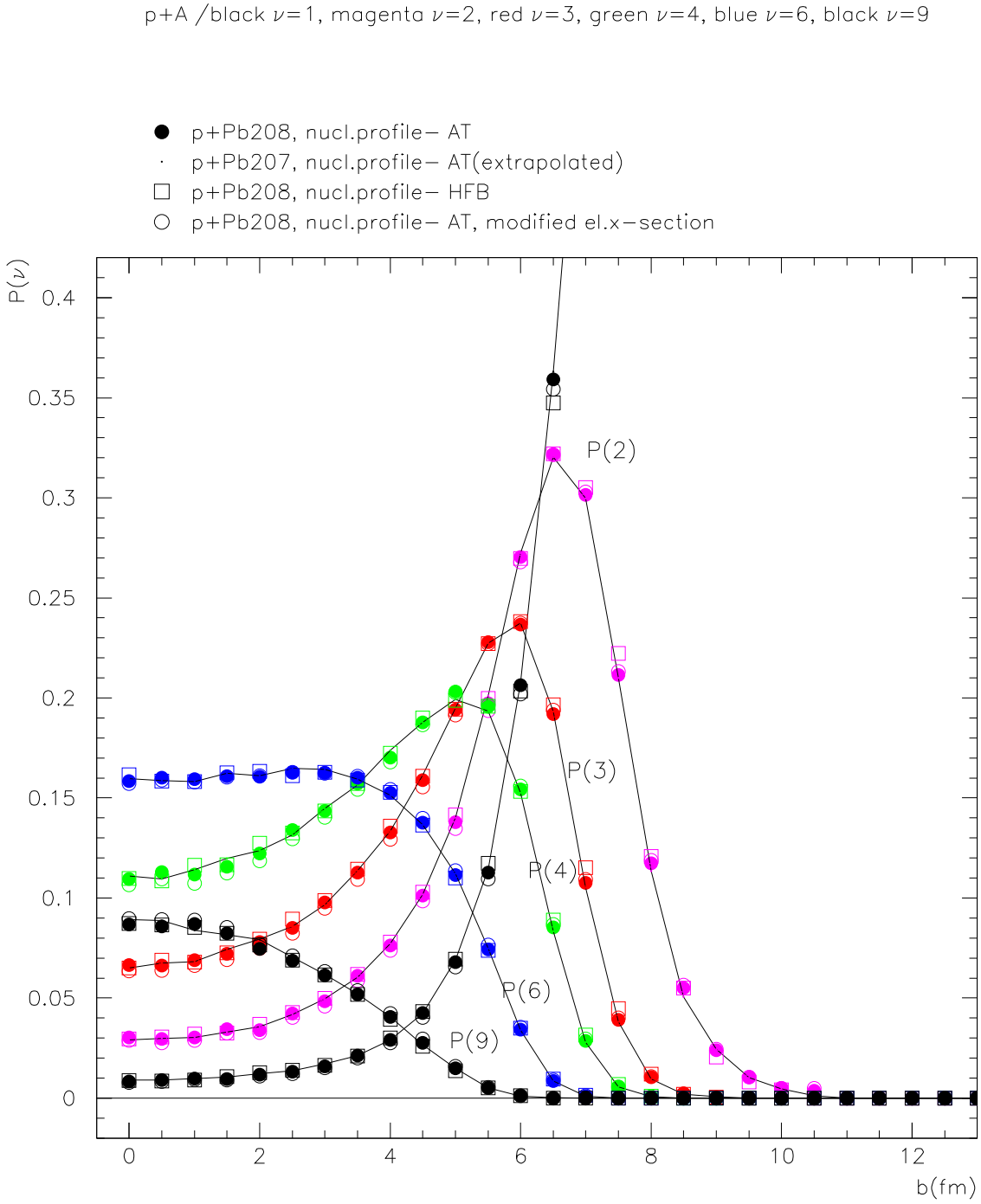

Figure 20: Impact parameter dependence of probabilities $P(1)$, $P(2)$, $P(3)$, $P(4)$, $P(6)$, and $P(9)$ for the p+Pb reaction *(magnified plot)*. The four Monte-Carlo options discussed in Sec. 15 are displayed by means of different symbols.

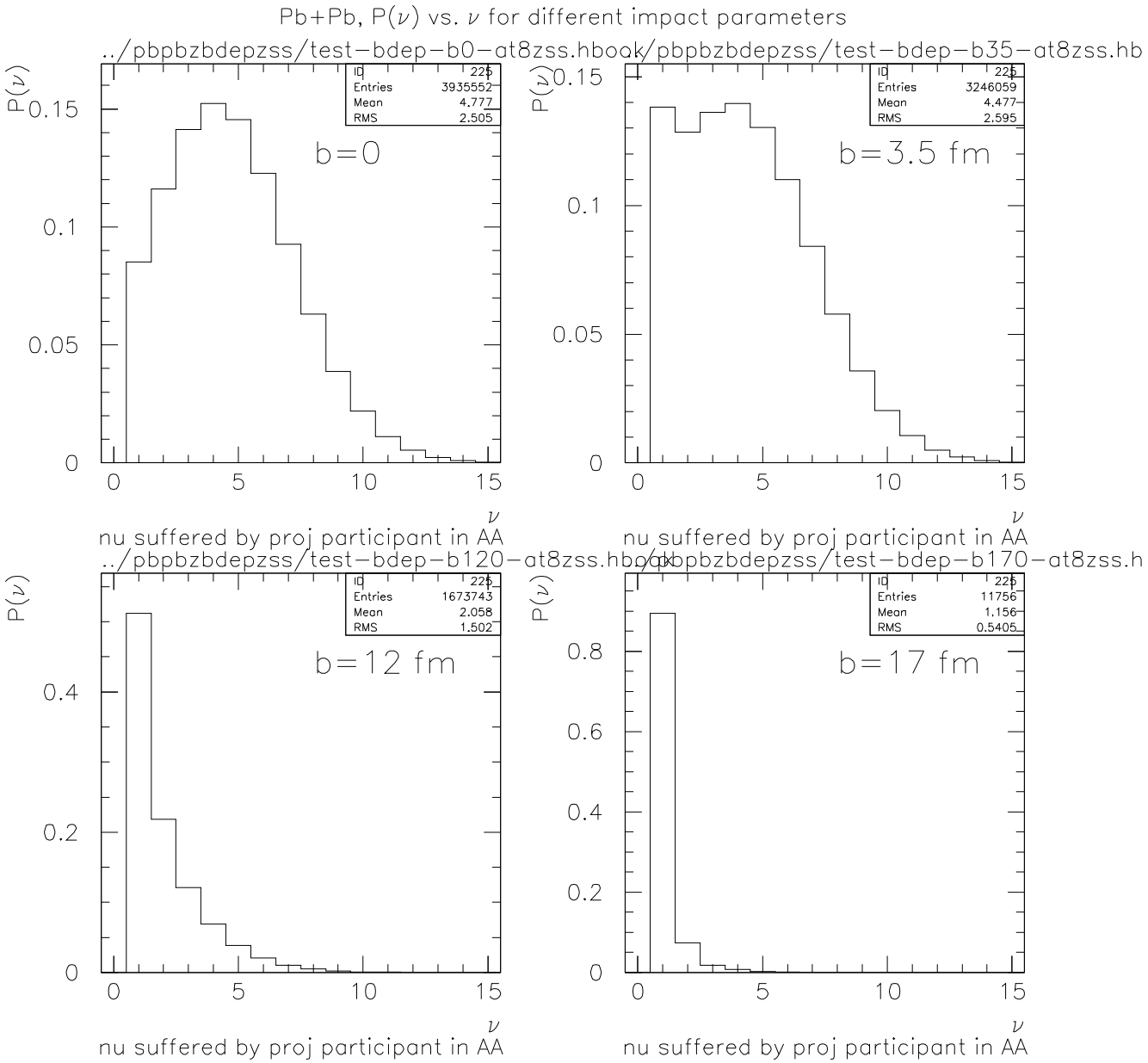

Figure 21: Distributions of probability $P(\nu)$ for the Pb+Pb reaction occurring at an impact parameter of 0, 3.5, 12 and 17 fm. The distributions correspond to simulations made assuming the elementary cross section of 31.42 mb, the "AT" nuclear profile [10], and the ^{208}Pb nucleus.

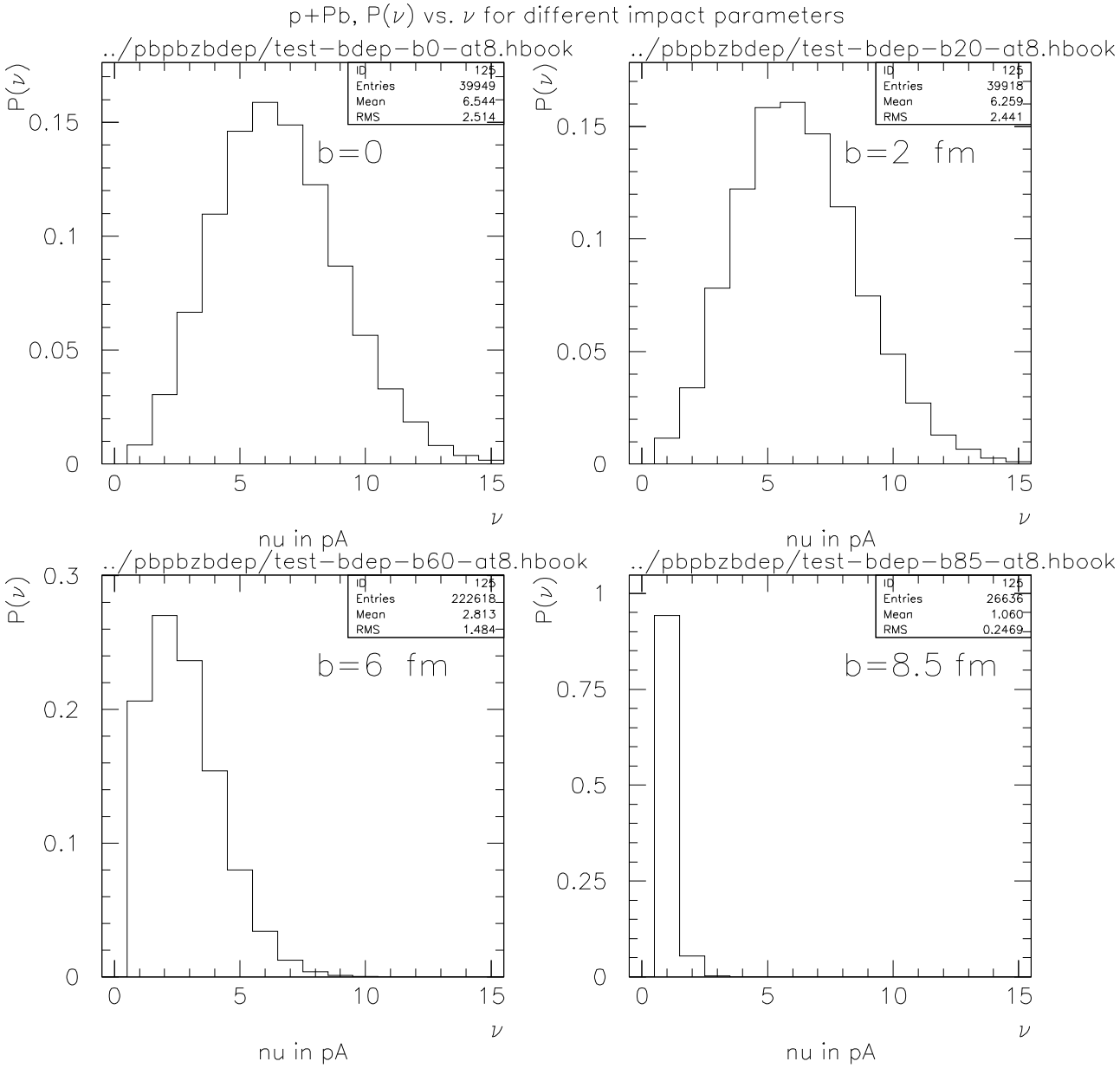

Figure 22: Distributions of probability $P(\nu)$ for the p+Pb reaction occurring at an impact parameter of 0, 2, 6 and 8.5 fm. The distributions correspond to simulations made assuming the elementary cross section of 31.42 mb, the "AT" nuclear profile [10], and the ^{208}Pb nucleus.

17 Mean Number of Elementary Collisions

The impact parameter dependence of the mean number $< \nu >$ of elementary collisions undergone by each nucleon participating to the Pb+Pb reaction, and by the projectile nucleon in the p+Pb reaction, is shown in Fig. 23. Similarly to the precedent Section, the spread induced by the different Monte-Carlo input parameters is small, indicating the value of $< \nu >$ is well defined. As said before, Pb+Pb reactions at $b = 0$ are characterized by a lower effective centrality relative to corresponding p+Pb collisions; the two $< \nu >$ values become equal only at an impact parameter of about 5 fm.

18 Number of Participating Nucleons, Protons and Neutrons

For reference in view of future studies, the present report also includes the dependence of the number of participating nucleons (protons, neutrons) on the impact parameter of the Pb+Pb reaction. This is shown in Figs 24 and 25 respectively on linear and logarithmic scales. Again, the uncertainties induced by the different Monte-Carlo input parameters (options **1-4** from Sec. 15) appear small.

19 Neutron Halo Effects

19.1 Pb+Pb Reactions

Fig. 26 shows the ratio of participating projectile neutrons over participating projectile protons as function of the impact parameter of the Pb+Pb reaction. The four options enumerated in Sec. 15 are considered. For the three options corresponding to the ^{208}Pb+^{208}Pb collisions (**1, 3, 4**) the ratio is below the nominal value of (126 neutrons)/(82 protons) for central reactions. The ratio reaches this nominal value at about $b = 8.5$ fm and then steeply increases. A similar behaviour is observed for the considered case of the ^{207}Pb+^{207}Pb collision (option **2**), but here the nominal ratio of 125/82 is the evident reference line[9].

The high value of the participating neutron/proton ratio at large impact parameter is expected as a direct consequence of the neutron halo effect. On the other hand, the opposite effect at $b = 0$ means that for central Pb+Pb collisions, where "nearly all" nucleons are supposed to participate, the collision is "loosing" more peripheral neutrons than protons. The effect is about -0.025 on the ratio. It is differently quantified in Fig. 27, where the number of neutrons "lost" or "gained" by a given impact parameter Pb+Pb collision, relative to the nominal value (N(participants)·126/208 or N(participants)·125/207) is shown. Again the options **1-4** coincide suggesting that this number is defined with a reasonable precision. It appears to be about 0.7 neutrons "lost" at $b = 0$. This evidently corresponds to 0.7 protons "gained" as illustrated in Fig. 27 on the unique example of the ^{207}Pb+^{207}Pb reaction. For large impact parameters ($b > 10$ fm), this number is only 0.2 as here the total number of participating nucleons is smaller (Figs 24-25).

Another issue to be taken note of is that for the range of impact parameters accessible to heavy ion experiments, the deviation of the neutron/proton ratio from the nominal value can be quantified within reasonable error limits. For instance, at $b = 10.5$ fm, this deviation would reach $+0.028 \pm 0.007$ following the present study.

[9] Further problems specific to ^{207}Pb+^{207}Pb reactions will be discussed in Sec. 20.

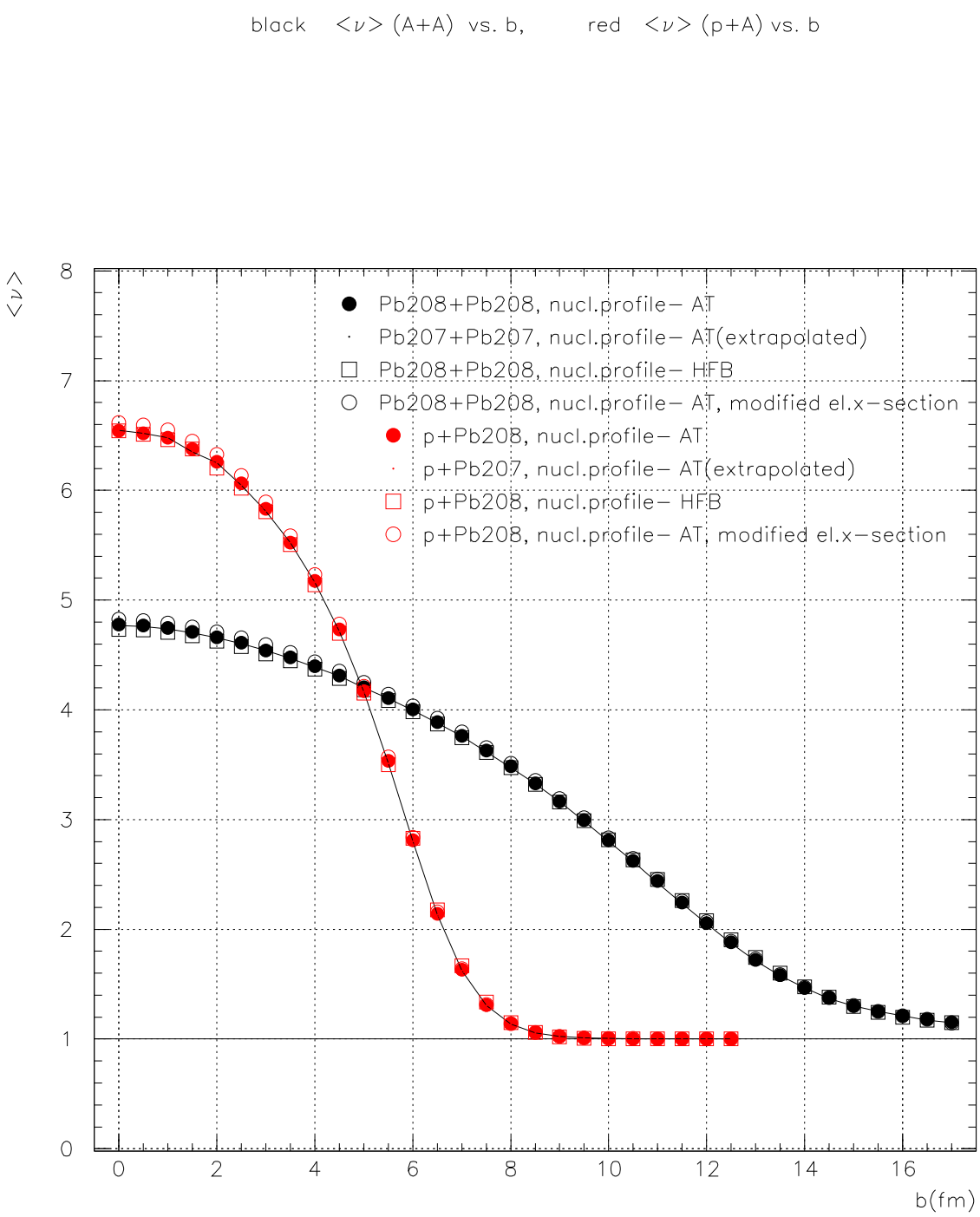

Figure 23: Mean number $< \nu >$ of elementary collisions in a Pb+Pb (black) and P+Pb (red) reaction, drawn as function of impact parameter. The four Monte-Carlo options discussed in Sec. 15 are displayed by means of different symbols.

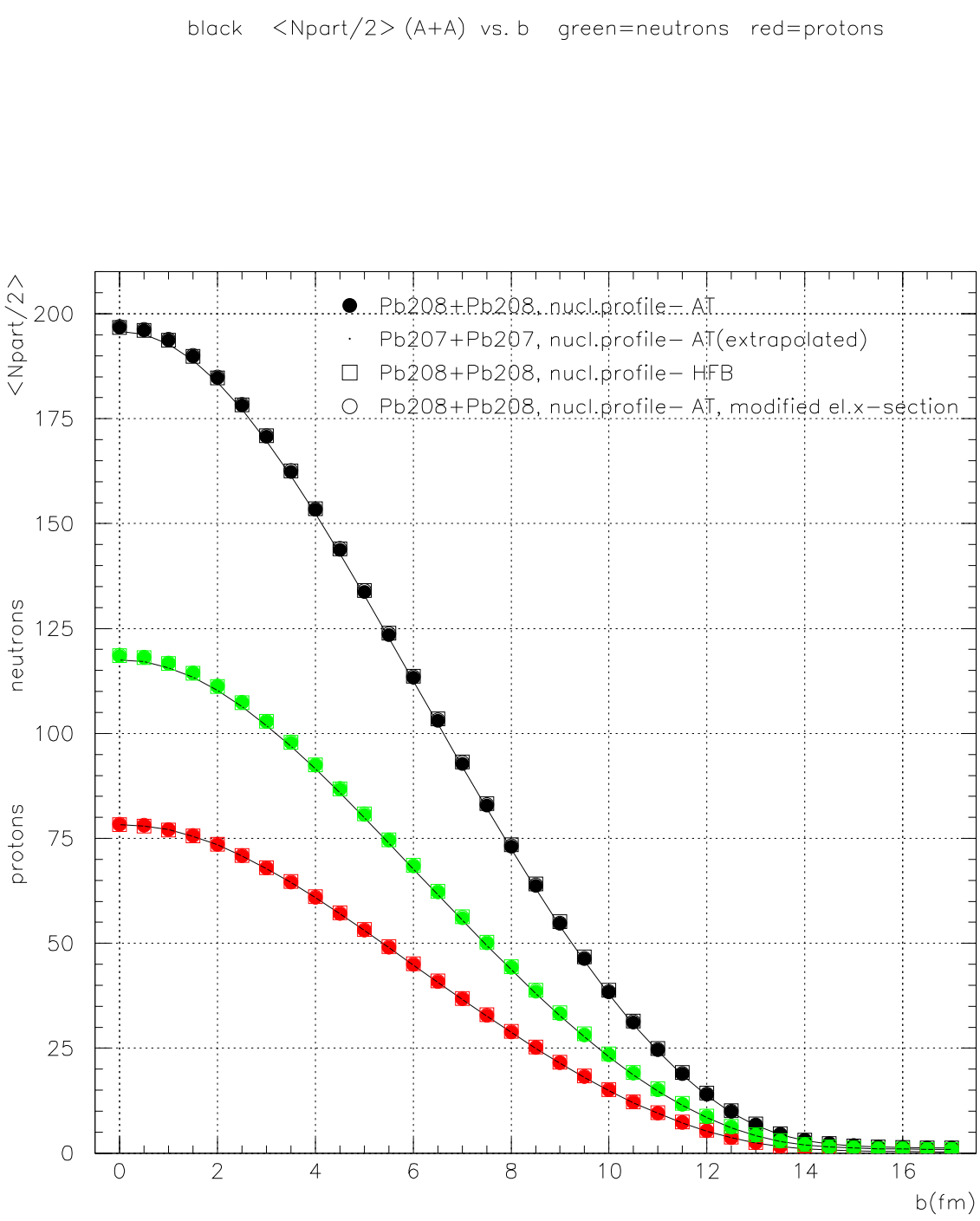

Figure 24: Mean number of projectile nucleons (black), projectile protons (red), and projectile neutrons (green) participating to the Pb+Pb reaction, drawn as function of the impact parameter *(linear plot)*. The mean number of participating projectile nucleons is equal to half the total mean number of participants (<Npart/2>). The four Monte-Carlo options discussed in Sec. 15 are displayed by means of different symbols.

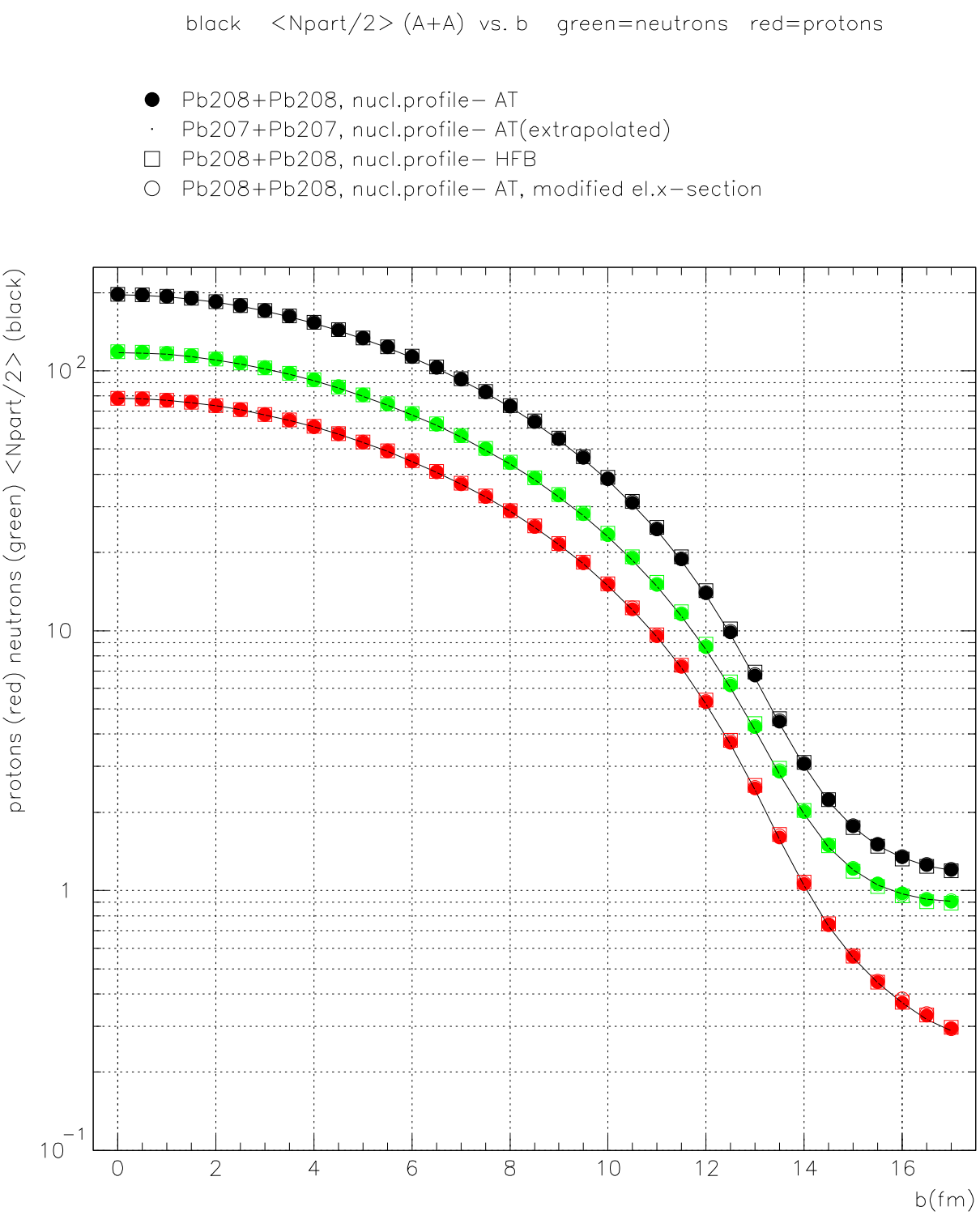

Figure 25: Mean number of projectile nucleons (black), projectile protons (red), and projectile neutrons (green) participating to the Pb+Pb reaction, drawn as function of the impact parameter *(logarithmic plot)*. The mean number of participating projectile nucleons is equal to half the total mean number of participants (<Npart/2>). The four Monte-Carlo options discussed in Sec. 15 are displayed by means of different symbols.

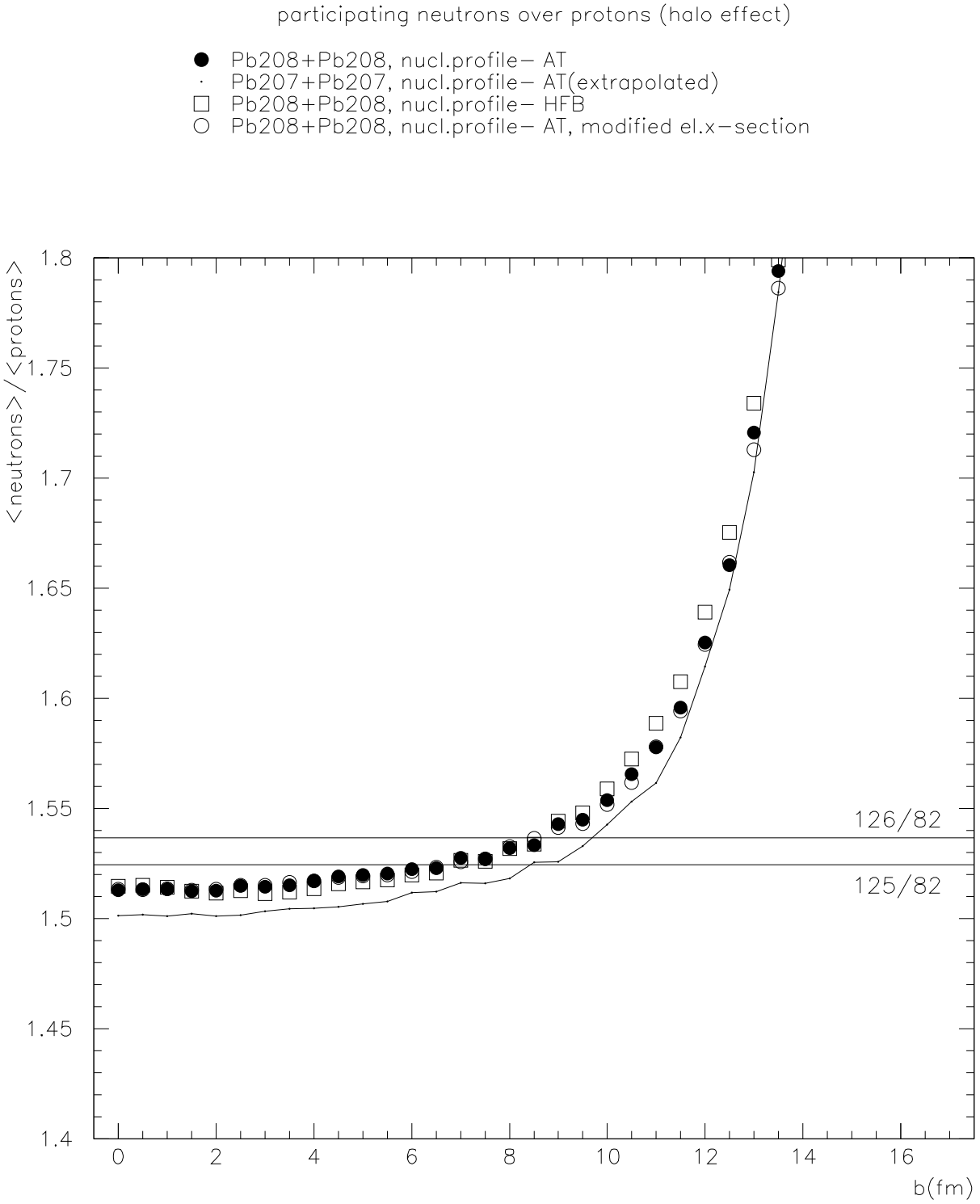

Figure 26: Ratio of participating projectile neutrons over participating projectile protons as function of the impact parameter of the Pb+Pb collision. The four Monte-Carlo options discussed in Sec. 15 are displayed by means of different symbols. The horizontal reference lines correspond to the nominal neutron/proton ratio of $126/82 \approx 1.537$ in ^{208}Pb nuclei, and to the nominal ratio of $125/82 \approx 1.524$ in ^{207}Pb nuclei.

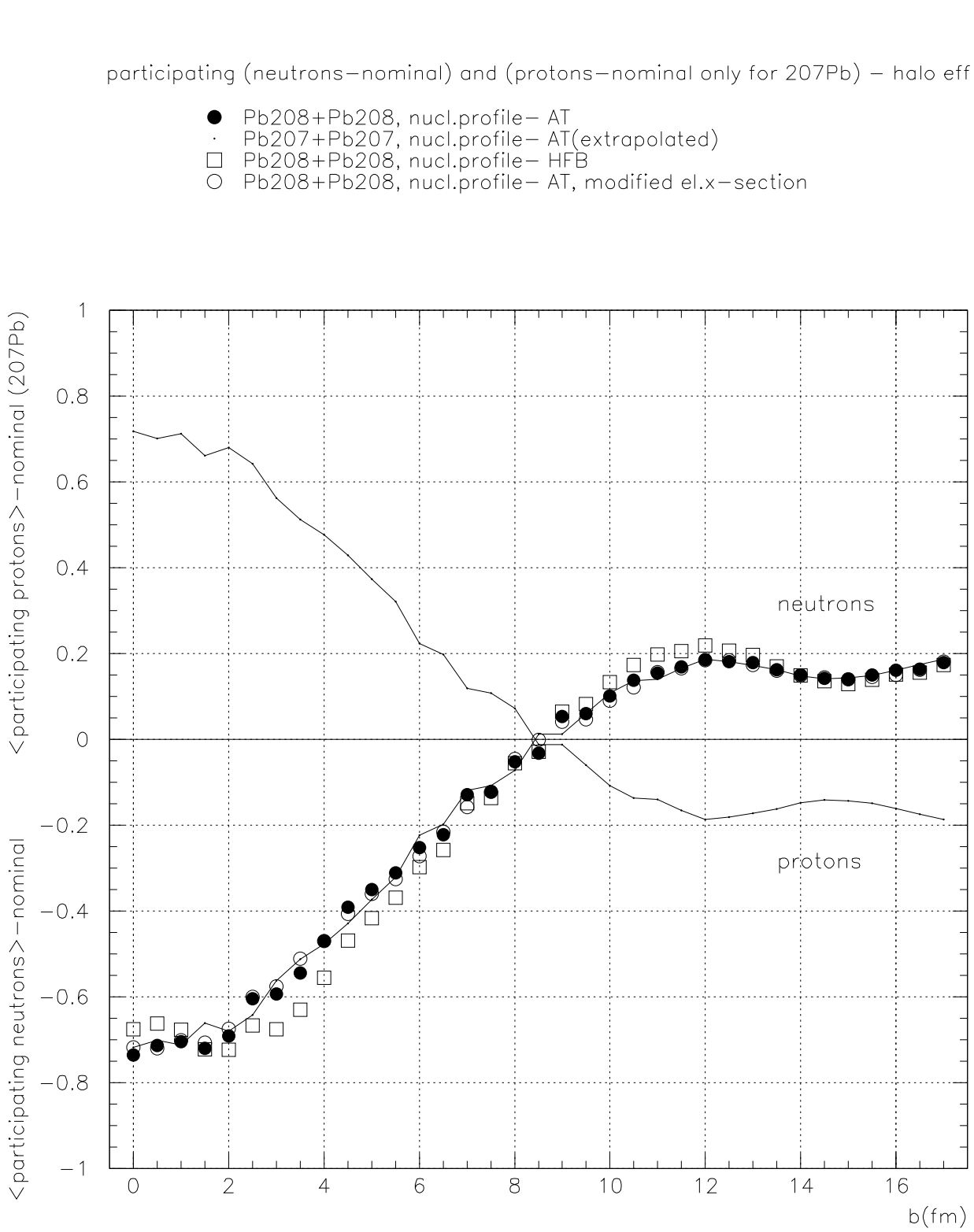

Figure 27: Impact parameter dependence of the number of participating projectile neutrons "lost" or "gained" by the Pb+Pb reaction relative to the nominal value, expected from the overall neutron/proton ratio in the nucleus. The four Monte-Carlo options discussed in Sec. 15 are displayed by means of different symbols. The number of participating protons is also illustrated on the unique example of the ^{207}Pb+^{207}Pb collision (option **2**, solid).

19.2 p+Pb Reactions

In Fig. 28, the participating neutron/proton ratio from Fig. 26 is compared to the ratio of target neutrons over target protons hit by the projectile in a p+Pb reaction. As a single projectile proton constitutes a "more precise probe" of the composition of the target nucleus, effects seen for p+Pb reactions are similar but larger relative to these seen in Pb+Pb collisions.

It is on the other hand to be remembered that even for p+Pb reactions, the influence of the nuclear profile's shape on the number of participating protons and neutrons is very strongly smeared by other factors. This is illustrated in Fig. 28 where the neutron/proton ratio as coming directly from the "HFB" profile [20] is plotted for comparison. The local structures present in this profile reflect very weakly, if at all, in the corresponding final hit target neutron/proton ratio (option **3**, open red squares).

For completeness, Fig. 29 shows the comparison between the number of participating neutrons "lost" or "gained" in the Pb+Pb collision relative to the nominal value (Sec. 19.1), and the number of target neutrons hit by the projectile in a p+Pb collision, again "lost" or "gained" relative to the nominal value. The different geometry of the p+Pb reaction results in a different quantitative size of the effect, corresponding to about 0.06 neutrons "lost" at $b = 0$ and to a maximal value of 0.4 neutrons "gained" at very large impact parameters (where essentially only neutrons are hit).

20 Comments

The principal goal of the study presented here was to provide reference data in view of future studies of the centrality dependence of Pb+Pb and p+Pb collisions. As such, the present Chapter does not require a specific summary. On the other hand, a few comments are to be taken into account in any future analysis.

Assumptions made on the ^{207}Pb nucleus. As said in Sec. 11.3, the nuclear profile of ^{207}Pb has been constructed by assuming the ^{208}Pb nuclear profile [10] extrapolated down to $A = 207$ by means of the general $R \sim A^{\frac{1}{3}}$ parametrization (that is, scaling down the proton and neutron half-density radii).

In view of the principal purpose - estimating the influence of the natural NA49 target on such centrality parameters as $< \nu >$, $P(\nu)$, or the mean number of participants - this approach is most probably reasonable. It may be somehow problematic in view of the analysis of neutron halo effects on the participating neutron/proton ratio. As such, the quantitative results obtained for ^{207}Pb+^{207}Pb or p+^{207}Pb reactions (Figs 26-29) are to be seen with some caution.

On the other hand, corresponding NA49 studies focus on the projectile hemisphere [25]. Here, the participating projectile nucleons belong exclusively to the ^{208}Pb nucleus for which no extrapolation is required.

General remark on nuclear profiles from antiprotonic atom data. As quantified in [8], the antiprotonic atom data probe the relative proton and neutron content only at the extreme periphery of the Pb nucleus. For future studies, it might be useful to include data obtained for pionic atoms, which probe a deeper region of the nucleus [26], into considerations on nuclear profiles and their influence on particle production.

Final comment on statistics. For possible future reference, the size of the statistical samples used for the simulations made in the present Chapter is graphically documented in Fig. 30. It is quantified by the total number of participating nucleons in Pb+Pb reactions, and by the total number of events in p+Pb collisions. Note that the p+Pb statistics is multiplied by 10 for the

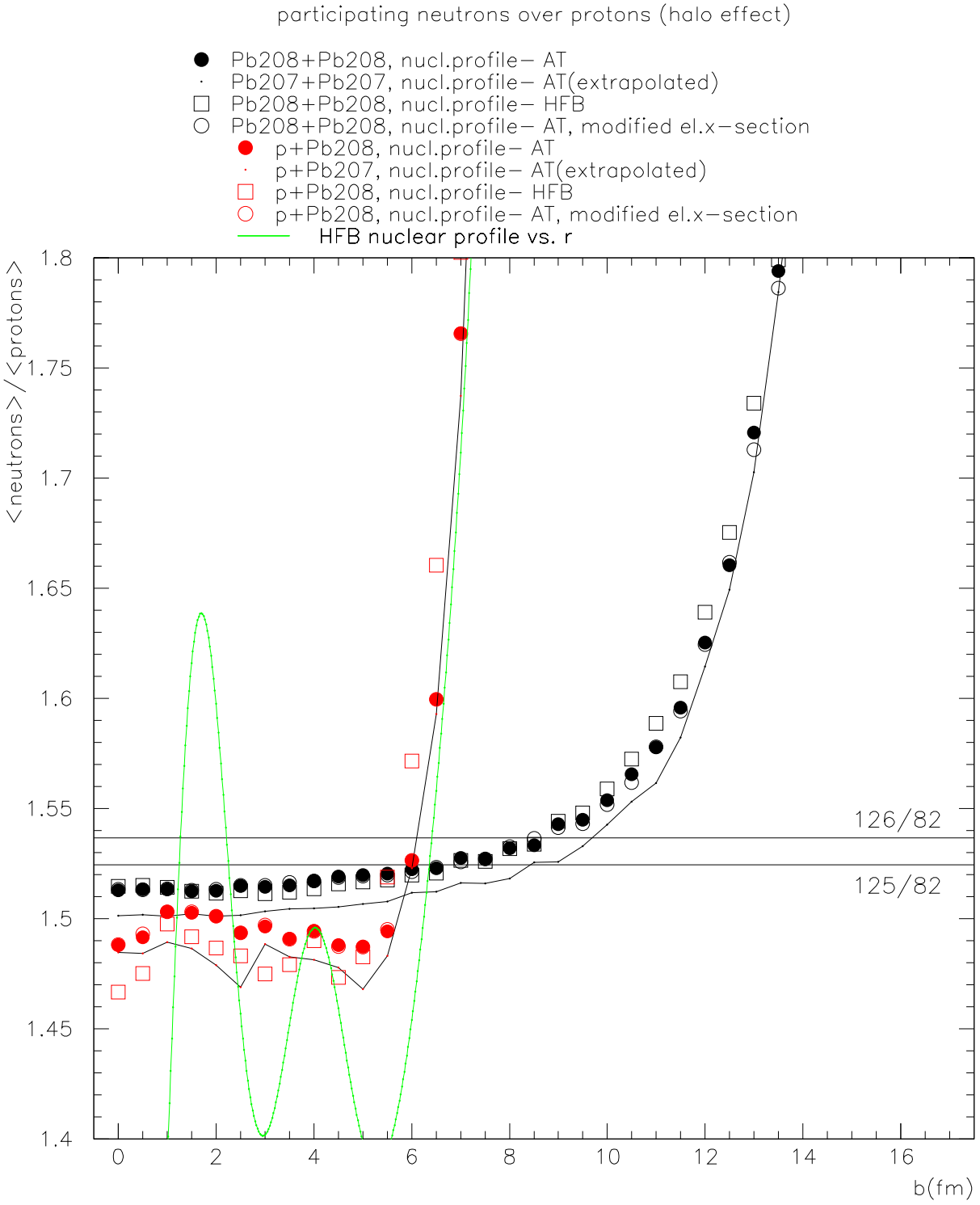

Figure 28: *Red symbols*: ratio of target neutrons over target protons hit by the projectile in the p+Pb reaction, drawn as function of impact parameter. *Black symbols*: ratio of participating projectile neutrons over participating projectile protons in the Pb+Pb collision. The four Monte-Carlo options discussed in Sec. 15 are displayed by means of different symbol types. The horizontal reference lines correspond to the nominal neutron/proton ratio of $126/82 \approx 1.537$ in ^{208}Pb nuclei, and to the nominal ratio of $125/82 \approx 1.524$ in ^{207}Pb nuclei. The solid green curve corresponds to the neutron/proton density ratio $\rho_{neutron}(r)/\rho_{proton}(r)$ drawn as function of the nuclear radius, as coming from the "HFB" profile [20].

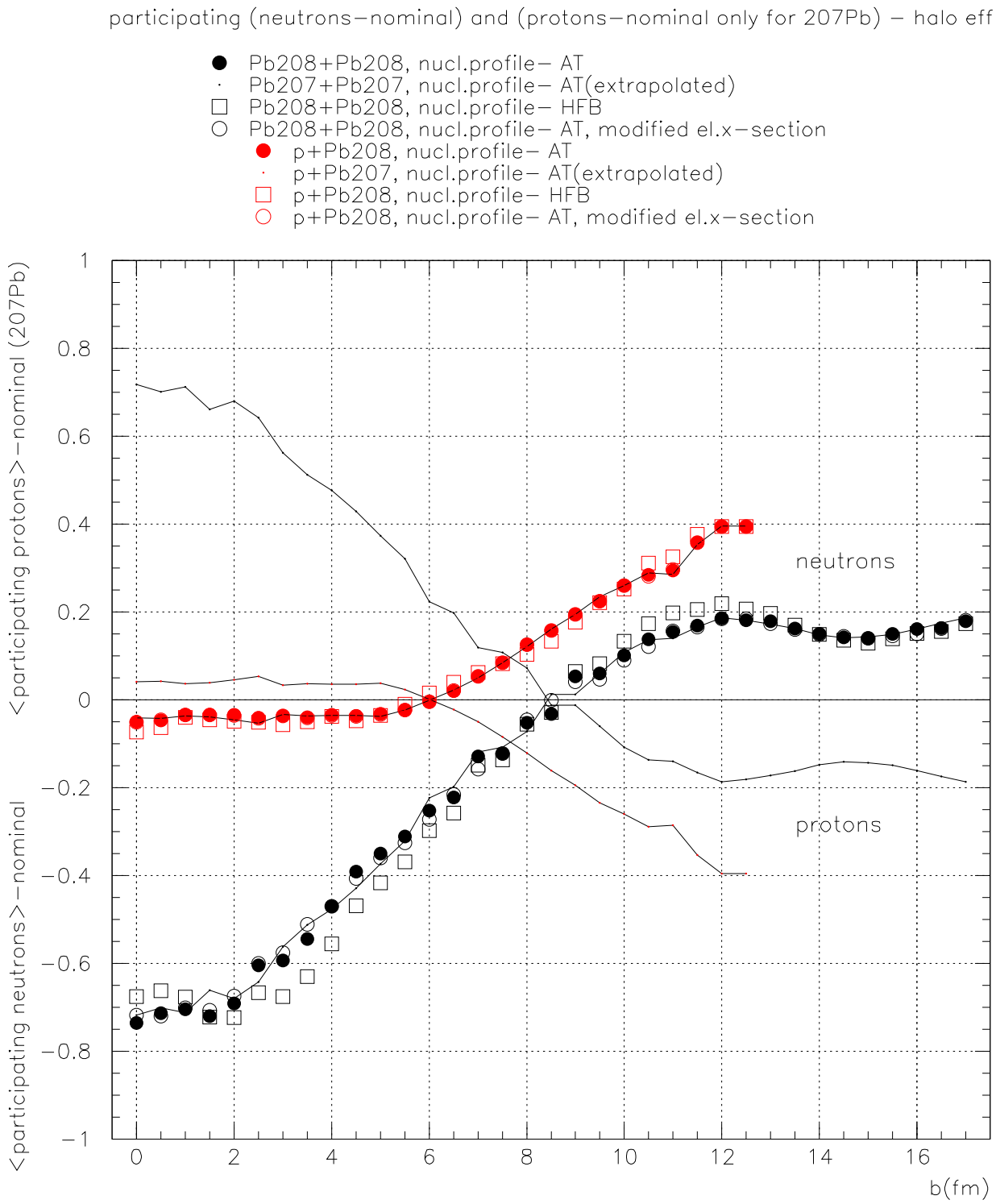

Figure 29: *Red symbols*: impact parameter dependence of the number of target neutrons hit by the projectile in the p+Pb reaction, "lost" or "gained" relative to the nominal value, expected from the overall neutron/proton ratio in the nucleus. *Black symbols*: impact parameter dependence of the number of participating projectile neutrons, "lost" or "gained" by the Pb+Pb reaction relative to the nominal value. The four Monte-Carlo options discussed in Sec. 15 are displayed by means of different symbol types. The number of "lost" or "gained"protons is also illustrated on the examples of the p+^{207}Pb and ^{207}Pb+^{207}Pb reactions (solid curves).

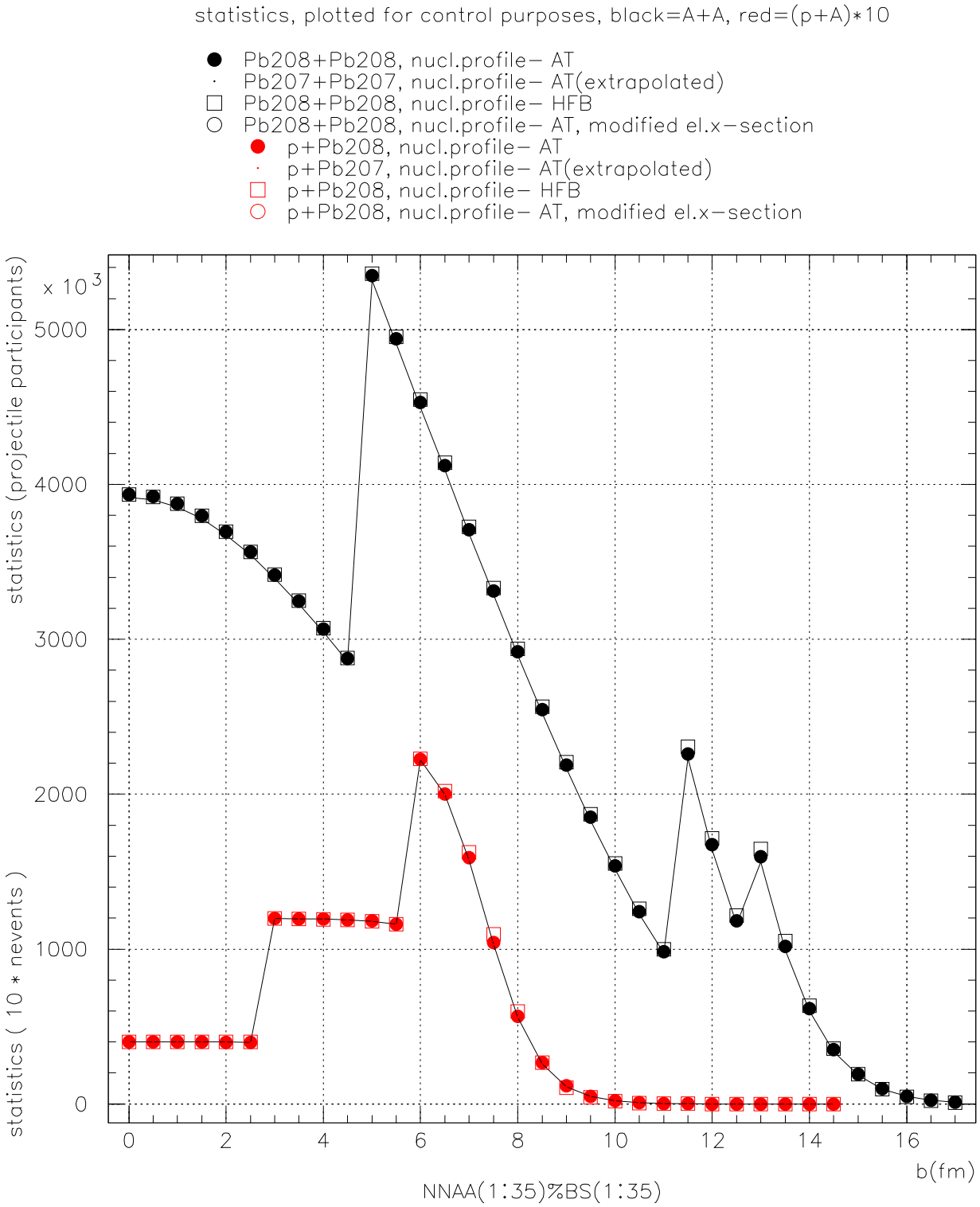

Figure 30: Size of the statistical Pb+Pb (black) and p+Pb (red) Monte-Carlo samples used in the present analysis. The four options discussed in Sec. 15 are displayed by means of different symbol types. Each Monte-Carlo sample is defined by the assumed impact parameter b. The statistics of each sample is quantified by the total simulated number of participating nucleons (in Pb+Pb reactions) or by the total number of interaction events (in p+Pb reactions). Note that the p+Pb statistics is multiplied by 10 for presentation purposes.

clarity of the presentation.

Part IV
Acknowledgments

Extremely valuable help coming from Agnieszka Trzcińska is kindly acknowledged. Many thanks are due to Jerzy Bartke, Antoni Szczurek and Jacek Okołowicz for their valuable remarks, and to Ewelina Kornaś for her help in scanning figures from literature. Last but not least, many thanks to Martin Makariev and to Hans Gerhard Fischer for inspiring the various parts of the whole study and for providing useful information.
This work was supported by the Polish State Committee for Scientific Research under grant no. 1 P03B 097 29.

Note: full information resulting from this analysis, numerical results, etc, will remain available. Information on computer data files, plots, text outputs, will remain present in files ~/pc/pcnote1.ps and ~/p1analysis/for-bdep/p1description.txt.

References

[1] NA49 Collab., S. Afanasev et al., Nucl. Instrum. Meth. A 430 (1999) 210.

[2] PHOBOS Collab., B. B. Back et al., Phys. Rev. C 65 (2002) 031901.

[3] Preliminary plot by Martin Makariev, private communication. Final data to be found in ref. [17].

[4] H. G. Fischer, NA49 Collab., Nucl. Phys. A 715 (2003) 118c.

[5] G. Barr, O. Chvala, H. G. Fischer, M. Kreps, M. Makariev, C. Pattison, A. Rybicki, D. Varga, S. Wenig, "Charged Pion Production in p+C Collisions at 158 GeV/c Beam Momentum: Discussion", submitted to Eur. Phys. J. C, arXiv:hep-ex/0606029.

[6] NA49 Collab., C. Alt et al., Eur. Phys. J. C 45 (2006) 343, and references therein.

[7] A.Trzcińska, private communication.

[8] A.Trzcińska et al., Phys. Rev. Lett 87 (2001) 082501.

[9] H. Enge, "Introduction to Nuclear Physics", Addison-Wesley World Student Series edition, 1972, and references therein.

[10] A.Trzcińska, Ph.D. Thesis, Heavy Ion Laboratory, Warsaw University, May 2001; http://www.slcj.uw.edu.pl/∼agniecha/phthesis_at.ps.gz (*in Polish*).

[11] A. Strzałkowski, "Wstęp do fizyki jądra atomowego", Państwowe Wydawnictwo Naukowe, Warsaw 1978 (*in Polish*).

[12] J. Bartke, private communication.

[13] Model independent analysis in:
E. A. J. M. Offermann et al., Phys. Rev. C 44 (1991) 1096.

[14] Model independent analysis as quoted in ref. [16]:
I. Sick, Phys. Lett 116B (1982) 212, and private communication.
Datasets included as quoted by ref. [16]:
I. Sick and J. S. McCarthy, Nucl. Phys. A 150 (1970) 631;
J. A. Jansen et al., Nucl. Phys A 188 (1972) 337;
G.Fey, Master's thesis, Technische Hochschule Darmstadt, 1973 (unpubl.);
L. S. Cardman et al., Phys. Lett. 91B (1980) 203.

[15] Discussion made in: G.Fricke et al, Atomic Data and Nuclear Data Tables (ADNDT) 60 (1995) 177;
method introduced by: B.Dreher et al., Nucl. Phys. A 235 (1974) 219.

[16] Discussion made in: H.de.Vries ADNDT 36 (1987) 495;
method introduced by: I.Sick, Nucl. Phys. A 218 (1974) 509.

[17] NA49 Collab., C. Alt *et al.*, "Inclusive production of charged pions in p + C collisions at 158-GeV/c beam momentum", submitted to Eur. Phys. J. C, arXiv:hep-ex/0606028.

[18] S. Fredriksson, G. Eilam, G. Berlad and L. Bergstrom, "High-Energy Collisions With Atomic Nuclei. Part 1", TRITA-TFY-84-06, May 1984.

[19] H. G. Fischer, NA49 Collab., Acta Phys. Polon. B 33 (2002) 1473;
A. Rybicki, J. Phys. G 30 (2004) S411;
A. Rybicki, Acta Phys. Pol. 35 (2004) 145;
O. Chvala, NA49 Collab., Eur. Phys. J. C 33 (2004) S615.

[20] S. Mizutori et al., Phys. Rev. C63 (2001) 025501.

[21] G. E. Cooper, "Baryon stopping and hadronic spectra in Pb Pb collisions at 158-GeV/nucleon", LBNL-45467.

[22] O. Chvala, private communication.

[23] P. Pawłowski and A. Szczurek, Phys. Rev. C 70 (2004) 044908.

[24] A. Rybicki, NA49 Collab., Acta Phys. Polon. B 33 (2002) 1483.

[25] A. Rybicki, J. Phys. G 30 (2004) S743.

[26] E. Friedman, private communication.